



Deliverable n°4.2.1

TECHNICAL REPORT ON VIBRATION PERFORMANCE

03/2022

University of Portsmouth



European Regional Development Fund



**WP T4: Production of a natural biaxial fabric and integration of its composites
in a sailboat hydrofoil**

**Act 2: Analysis of the influence of flax fibres on the vibration behaviour of the
composite material**

(Deliverable 1: Technical report on vibration performance)

**Vibration damping behaviour of flax fibre reinforced epoxy and its carbon
fibre hybrid composites: experimental investigation and numerical analysis**

**Moumita Sit, Saeid Dashatan, Jérémy Millot, Zhongyi Zhang, Erwan Grossmann, Hom N
Dhakal**

School of Mechanical and Design Engineering

University of Portsmouth, Portsmouth UK





Abstract

This technical workpackage investigated the vibration damping properties of flax fibre reinforced epoxy composites and its carbon/flax hybrid composites. Flax and flax/carbon hybrid composite laminates were fabricated by Kairos, the lead partner for the WP T4 with various orientations of reinforcing layers. The dynamic properties were then determined from the vibration measurements of beam test specimens and Derritron VP85 shaker. The frequency response of a sample was measured and the response at resonance was used to estimate the natural frequency and damping loss factor. Experiments were subsequently conducted on a range of samples with different geometry and fibre layup. Numerical estimates of the response, and in particular the natural frequencies, were made using the analytical solution of cantilever Euler-Bernoulli Beam and modal analysis in finite element modelling in Abaqus software. In analytical results, all the beam parameters like modulus of elasticity and density are extracted from the nominal material properties for individual laminas from a specific layup for each specimen. The experimental results showed that among the tested composite and hybrid composites, the highest damping ratio of flax-epoxy composites where flax fabrics were placed in outer layers of composites. The experimental results showed good agreement with the numerical results confirming the accuracy of the results. The findings from this work indicate that the flax fibre reinforced composites could be a commercially viable material for applications where vibrational excitation are subjected in their service conditions and high vibrational damping is required.

Keywords: Flax fibre; Bio-based composites; Vibration damping; Numerical modelling.



Contents

Abstract.....	3
List of Figures	5
List of Tables	7
1 Introduction	8
2 Experimental Procedure	10
2.1 Shaker system	10
2.2 Sensors.....	11
2.3 Material.....	12
3 Theory	16
4 Results and Discussion	19
4.1 Calibration results and Input parameters.....	19
4.2 Aluminum alloy beam as the reference material: Case 1	20
4.3 Aluminum alloy beam as the reference material: Case 2	24
4.4 Aluminum alloy beam as the reference material: Case 3	29
4.5 Test on flax/carbon hybrid epoxy beam	32
4.6 Test on flax/epoxy composite beam 1: Case 1	36
4.7 Test on flax/epoxy composite beam 1: Case 2	40
4.8 Test on flax/epoxy composite beam 2: Case 1	45
4.9 Test on flax/epoxy composite beam 2: Case 2	48
4.10 Test on flax/carbon hybrid composite beams (2 nd batch of samples).....	53
5 Conclusions	58
References	59
Appendix A:.....	61
Appendix B:	63
Appendix C:	69



List of Figures

Figure 1. (a) B&K accelerometer type 4507; (b) B&K accelerometer type 4517	11
Figure 2. Experimental setup for vibration test (a) with B&K accelerometer type 4507; (b) with B&K accelerometer type 4517	11
Figure 3. Infusion of the hybrid carbon-flax samples at Kairos' workshop	13
Figure 4. The 3 dB method diagram for calculating the damping factor Q	17
Figure 5. Experimental setup for aluminium alloy beam with B&K accelerometer type 4507 (a) top view; (b) side view	19
Figure 6. Transfer function for swept sine signal (10 Hz to 1000 Hz)	20
Figure 7. Transfer function for swept sine signal (a) 10 Hz to 50 Hz; (b) 100 Hz to 200 Hz; (c) 400 Hz to 500 Hz	21
Figure 8. Experimental setup for aluminium alloy beam with B&K accelerometer type 4517 at the tip	23
Figure 9. Transfer function for swept sine signal (10 Hz to 1200 Hz)	23
Figure 10. Transfer function for swept sine signal (a) 20 Hz to 30 Hz; (b) 165 Hz to 185 Hz; (c) 500 Hz to 520 Hz; (d) 990 Hz to 1020 Hz	26
Figure 11. Experimental setup for aluminium alloy beam with B&K accelerometer type 4517 near the clamped end	28
Figure 12. Transfer function for swept sine signal (10 Hz to 1200 Hz)	28
Figure 13. Transfer function for swept sine signal (a) 25 Hz to 35 Hz; (b) 175 Hz to 195 Hz; (c) 495 Hz to 520 Hz; (d) 950 Hz to 1010 Hz	31
Figure 14. Experimental setup for flax/carbon hybrid epoxy beam (a) top view; (b) side view	32
Figure 15. Transfer function for swept sine signal (100 Hz to 3000 Hz)	32
Figure 16. Transfer function for swept sine signal (a) 120 Hz to 150 Hz; (b) 840 Hz to 900 Hz; (c) 950 Hz to 1030 Hz; (d) 2400 Hz to 2560 Hz	34
Figure 17. Experimental setup for flax/epoxy composite beam 1: Case 1	35
Figure 18. Transfer function for swept sine signal (10 Hz to 1000 Hz)	36
Figure 19. Transfer function for swept sine signal (a) 15 Hz to 25 Hz; (b) 130 Hz to 150 Hz; (c) 360 Hz to 400 Hz; (d) 700 Hz to 740 Hz; (e) 750 Hz to 830 Hz	38
Figure 20. Experimental setup for flax/epoxy composite beam 1: Case 2	39
Figure 21. Transfer function for swept sine signal (10 Hz to 1000 Hz)	40
Figure 22. Transfer function for swept sine signal (a) 16 Hz to 26 Hz; (b) 130 Hz to 150 Hz; (c) 360 Hz to 390 Hz; (d) 680 Hz to 750 Hz; (e) 750 Hz to 830 Hz	42
Figure 23. First three frequencies of vibration for flax/epoxy composite (beam 1) calculated by Abaqus FEM	43
Figure 24. Experimental setup for flax/epoxy composite beam 2: Case 1	44
Figure 25. Transfer function for swept sine signal (10 Hz to 1500 Hz)	45



Figure 26. Transfer function for swept sine signal (a) 45 Hz to 65 Hz; (b) 950 Hz to 1090 Hz; (c) 360 Hz to 400 Hz	46
Figure 27. Experimental setup for flax/epoxy composite beam 2: Case 2	47
Figure 28. Transfer function for swept sine signal (10 Hz to 1500 Hz	48
Figure 29. Transfer function for swept sine signal (a) 50 Hz to 70 Hz; (b) 360 Hz to 400 Hz; (c) 950 Hz to 1050 Hz; (d) 1250 Hz to 1350 Hz	50
Figure 30. First three frequencies of vibration for flax/epoxy composite (beam 2) calculated by Abaqus FEM	51
Figure 31. Experimental setup for 2 nd phase of tests	52
Figure 32. Comparison of damping ratio and loss factor for different samples	55



List of Tables

Table 1.	Mass and geometry of test samples used in first phase	13
Table 2.	Mass and geometry of test samples used in second phase	14
Table 3.	Properties of individual lamina	16
Table 4.	Calculation of Young’s modulus of aluminium alloy using B&K accelerometer type 4507	22
Table 5.	Calculation of Young’s modulus of aluminium alloy using B&K accelerometer type 4517	27
Table 6.	Numerical result for the aluminium alloy cantilever beam	27
Table 7.	Resonance frequencies of different laminates obtained from experiment and numerical analysis	53
Table 8.	Damping ratios and loss factor calculated by 3dB method for different laminates	54



1 Introduction

The introduction of natural plant fibre composites (NPFs) over the last ten years has brought significant interest in key engineering applications such as automotive, marine and construction industries. Apart from being sustainable and biodegradable, NPFs offer several advantages such as low cost, light weight, low density, high specific strength and low abrasiveness compared to their conventional counterparts such as glass and carbon fibre reinforced composites. Moreover, the inherent damping property of natural bast plant fibres (flax, hemp, jute and kenaf) is a significant factor in controlling the resonance response and consequently helps in prolonging their service life under cyclic and impact loadings.

However, the application of the NPFs in structural components requires a thorough understanding of their material properties and mechanical performance. Although a number of reports on the manufacturing technique and the mechanical performance of the flax fibre reinforced composites are available in the published literature, only a few investigations can be observed related to the vibrational damping performance. In this report, natural frequencies and vibration damping properties of flax fibre reinforced biocomposites and hybrid flax/carbon fibre-reinforced composites are investigated and characterized experimentally and numerically.

Many engineering structures made from composites, including military equipment, automobiles, aircrafts, boat hulls, wind turbine blades and spacecrafts, encounter vibrational amplitudes during their service life. For example, the fatigue caused by vibration often leads to the initiation of micro-cracks in these structures, which propagate rapidly, consequently leading to premature failure [1]. Therefore, it is necessary to pay attention to the sound absorbing properties and the vibration damping behaviours of the composite structures subjected to various excitation scenarios, to reduce the effect of vibration and noise. At present, the common state-of-art methods involve improving the damping performances of the structures while retaining the other primary structural functions. Over the last couple of decades, there has been an increasing demand for more environmentally friendly materials [2]. In spite of having high tensile strength and stiffness, carbon and glass fibre reinforced composites have low damping coefficient [3–5]. Natural plant fibres such as hemp and flax, on the other hand, have a lower tensile strength than synthetic fibres such as glass and carbon [6–8], but have much higher damping properties [5,9] due to their hollow morphological



structure able to dissipate high energy. As a results of these inherent characteristics, NPFCs have the potential to overcome some critical problems, such as vibration damping properties that cannot be addressed by conventional composite materials in engineering structures. This fact leads to the idea of developing novel hybrid composites, where natural flax fibres can be combined with carbon fibres to produce new and advanced functionalities in structures [10]. In particular, natural plant fibres such as flax, present some key advantages over man-made fibres, including reduced occupational health issues in manufacturing, lower costs, potential lower environmental impact, and relatively good specific mechanical properties [11–13].

The key objectives of this present study is to evaluate the vibrational damping behaviour of flax fibre based epoxy composites and its carbon hybrid system by employing experimental and numerical approaches. For this, the stepped sine vibration test of flax and carbon hybrid cantilever beams were investigated using an electrodynamic shaker system which is capable to identify the main frequency responses of the shaker system and can identify the main modes and damping characteristics of a beam. For calibration purpose, an aluminium beam was used so as to identify a wide range of resonance frequencies from low, e.g. 10 Hz to high, e.g. 1000 Hz, frequency range due to the natural modes of the beam employed. The test protocol identified from the preliminary study on aluminium beam was applied to the natural-fibre composite specimens of various compositions and geometric shapes.

In order to compare and validate the experimental results, an analytical solution based on Euler-Bernoulli Beam theory was used. In addition to the analytical solution, the modal analysis Abaqus finite element analysis (FEA) software are used for the calculation of the first three natural frequency of the beams. Details of the analytical method is provided in sections in following sections.



2 Experimental Procedure

The frequencies and damping ratios were measured using the vibration cantilever beam method, with a Derritron VP85 shaker.

2.1 Shaker system

The Derritron Electronics Electro-magnetic shaker system (type VP85) is powered by a DataPhysics DSA5-1K power amplifier with 1000W of maximum power and is controlled by a DataPhysics Abacus and Quattro control and data acquisition module. The shaker is capable of peak-to-peak displacement of 2.54 cm between 5 and 10 Hz giving rise to a maximum acceleration of 1g at 5 Hz to 4.5g at 10 Hz; it is limited by a maximum velocity of 0.76 m/s between 10 and 120 Hz giving rise to a maximum acceleration of 4.5g at 10 Hz to 55g at 120 Hz; from 120 Hz to 3000 Hz, the system is limited by the maximum acceleration of 55g. The above estimation is based on a moving mass of about 6.15 kg. As the moving masses increases, the maximum acceleration reached at frequencies higher than 120 Hz will be reduced accordingly.

Due to the above shaker characteristics, for sine sweep, stepped sine and broadband random vibration tests, the shaker's control system requires much less effort to equalise and reproduce the desired signal on the moving armature at frequencies higher than about 120 Hz. The system will require about 10 to 30 s for particular frequencies at the lower frequency range 10 to 120 Hz. for example, a sine wave at 21 Hz has 7-8% error in magnitude, while this error is only 1-5% at other frequencies between 10 and 30 Hz. However, it is totally feasible to work around to avoid these 'shaker characteristic frequency spots' – let's call them 'shaker spots'. To do so, we proposed:

- 1) Once the test specimen is mounted on the shaker's moving platform (armature), we run a broad stepped sine test in the range 10 to 1000 Hz and 1000 to 2500 Hz to identify any of the 'shaker spots' and the main modes of the specimen. In this case we use a coarse linear frequency step of about 0.5-1 Hz for 10-1000 Hz range, and 2 Hz for 1000-2500 Hz.
- 2) Break down test frequency bands into much smaller chunks based on a) the 'shaker spots' using the input acceleration measured at the centre of the shaker moving platform – input, and b) the main natural modes of the specimen using the



acceleration measured at the moving tip of the specimen cantilever beam – output. If test specimen has natural frequency close to the ‘shaker spots’, to reduce the magnitude error around the shaker spots, an increased ‘time out’ setting is tried. This usually gives satisfactory results with magnitudes errors in 10%, but with increased testing time

- 3) Run the tests with the multiple bands with different frequency resolution to check that there is adequate number of data points for each resonance so as to estimate the damping or loss factor using either the half-power bandwidth method or the SDOF circle fit of each mode’s Nyquist plot.

A DataPhysics Mobilizer with stepped sine mode was utilised for signal generation, data acquisition and analysis. Two accelerometers were used. One accelerometer was attached on the moving tip of the beam to measure the dynamic response of the composite beam. Another accelerometer was attached on the shaker to control and obtain a constant acceleration (0.5 g) of the shaker.

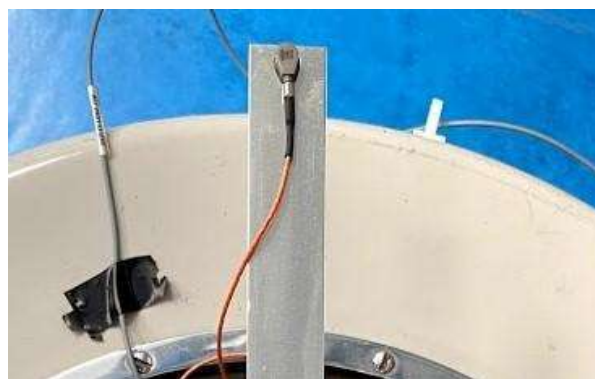
2.2 Sensors

Two types of accelerometers were used to record the response of the specimen.

1. B&K 4507 B ICP-type: Initially both accelerometers (specimen and shaker) were B&K 4507 B 006 ICP-type (Figure 1a). This accelerometer weighs 4.8 gm. However, the mass of this accelerometer was on the higher side compared to the mass of the specimen, which affected the damping property and Young’s modulus of the specimen.
2. B&K 4517 type: The accelerometer attached to the specimen was changed and B&K 4517 ICP-type (Figure 1b) accelerometer had been used instead. This accelerometer weighs 0.6 gm which is much lighter than the previous one and improved the experimental outcome.



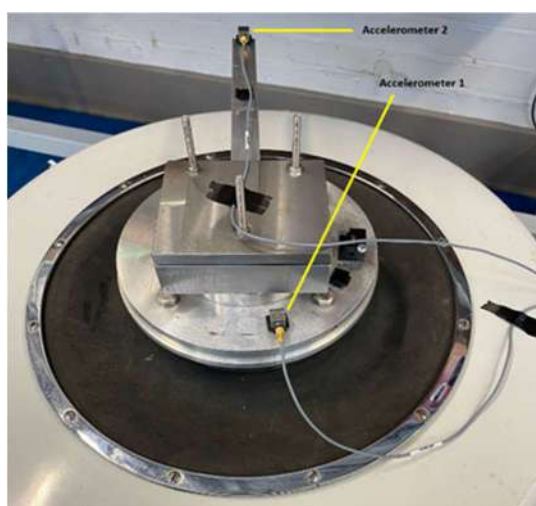
(a)



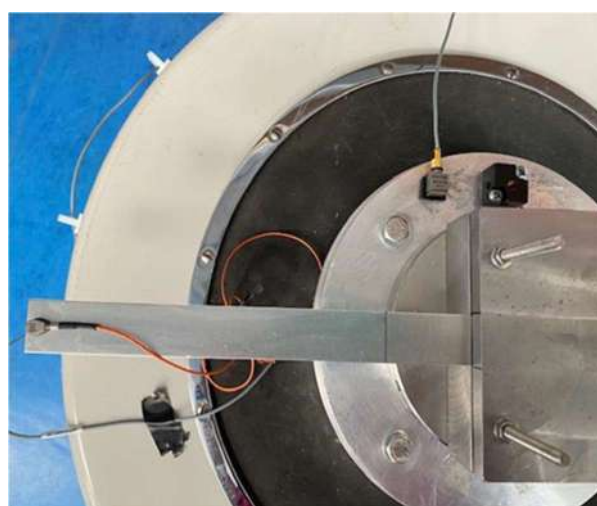
(b)

Figure 1. (a) B&K accelerometer type 4507; (b) B&K accelerometer type 4517

The whole experimental setups are shown in Figure 2.



(a)



(b)

Figure 2. Experimental setup for vibration test (a) with B&K accelerometer type 4507; (b) with B&K accelerometer type 4517

2.3 Material

The goal is to insert some flax fibers in a mostly unidirectional carbon fiber beam and find a good compromise between vibration absorption and mechanical properties loss. A set of eleven batches of samples has been designed and produced in order to test the influence of two parameters : flax fabric architecture and flax fabric position in the layup. Indeed these parameters have been identified in [14-15] as influential on vibration damping.



Three flax fabric architecture are tested :

*Unidirectional ('UD') with all fibers in the same direction. The commercial name is 'FlaxTape' from EcoTechnilin supplier.*Balanced ('EQ') with all fibers at 0/90° of fabric direction, 300 g/m². The commercial name is 'Amplitex' from Bcomp supplier.

*Biaxial ('BX') with all fibers at +-45° of fabric direction, 312 g/m². This fabric has been developed during FLOWER project with Depestele supplier.

Three flax position in the layup have been tested : outside layer "N" ; outside but one layer "N-1" and outside but two layer "N-2". By labeling 'C' a carbon ply and 'F' a flax ply it then gives 'CCCF' for 'N' configuration and 'CFCC' for 'N-2' configuration.

Two extra beams have been manufactured for reference of a carbon-only* beam and a flax-only beam (*to be able to compare it with other beams, there is actually flax in the core).

In order to be able to compare the vibration tests between all the samples, it has been decided to try to maintain similar geometry and mechanical traits between all the samples. Hence the samples are designed to have similar thickness, length and bending stiffness.

Maintaining a bending stiffness with the same thickness while adding a weaker ply on the outside (flax vs carbon) is a challenge. To achieve this, the samples are sandwich samples, and to compensate the reduction of stiffness from an outside flax layer, extra carbon plies are added towards the symmetry plane of the sandwich. But to maintain the same sandwich thickness, the core needs to reduce in thickness from the same thickness of these extra carbon plies. In order to avoid CNC machining of the core for removing tenths of millimeters, the core is made of several thin plies of flax. The hypothesis is that these plies are close to the neutral axis, hence they will perceive only tiny deformations and will not affect the damping.

These beams have been manufactured by vacuum-bag infusion process in a controlled temperature and air-moisture environment. Flax fabrics have been dried prior to layup, the resin (Sicommin Infugreen 810 + SD 8824 hardener bio-epoxy) was at room temperature before infusion. All the samples were infused at once next to each other as illustrated in Figure 3.

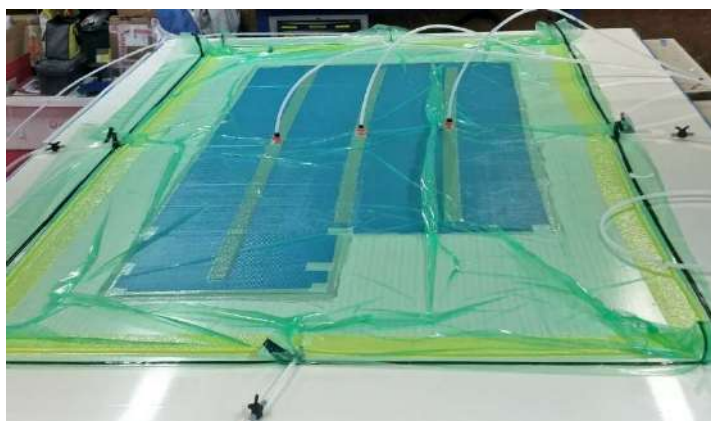


Figure 3 – Infusion of the hybrid carbon-flax samples at Kairos’ workshop.

Measuring vibration damping is not an easy task, many parameters influence the results, and the values measured are pretty small hence sensitive to noise. So before testing these complex flax-carbon sandwich composite beams, a simpler aluminum alloy (grade 6082 T6) beam has been used the reference material to identify the test protocols and the parameters. The same protocol has been used for the rest of the materials. The materials used in the first and second phases of experiments are listed in Table 1 and Table 2, respectively. The detailed layout of the samples are given in Appendix A.

Table 1. Mass and geometry of test samples used in first phase

Material	Mass (gm)	Length (mm)	Width (mm)	Thickness (mm)
1. Aluminium alloy Grade 6082 T6	20.18	240 Free length: 200 Root length: 40	21	1.45
2. Carbon-flax epoxy hybrid composite	35.04	240 Free length: 180 Root length: 60	20	5.20
3. Flax/epoxy composite (beam 1)	17.30	251 Free length: 200 Root length: 51	19	3.00
4. Flax/epoxy composite (beam 2)	11.6	168 Free length: 117 Root length: 51	19	3



Table 2. Mass and geometry of test samples used in second phase

Material	Fibre layup/stacking sequence	Length (mm)	Mass (gm)	Plate Thickness (mm)	Width (mm)
A1	CCCFC UD	Total length: 530 Free length: 450 Root length: 80	42.6	5.98	10.35
A4			41.6	5.87	10.35
B2	CCCCF 90		45.9	6.14	11.7
B3			43.5	6.02	11.3
C1	CCCCF UD		43.3	5.33	11.43
C4			43.4	5.4	11.43
D1	CCCCF 45		43	5.7	11.4
D3			44.2	5.74	11.5
E2	CCCFC 45		40.63	6.02	9.83
E3			40.58	6.15	9.84
F2	CCFCC 90		41.5	6.3	9.83
F4			40.76	6.2	9.83
G1	CCFCC 45		41.6	6.37	9.72
G3			41.4	6.34	9.75
H3	CCFCC UD		36.8	5.41	9.83
H4			38.3	5.6	9.7
I3	CCCFC 90	40.8	6.15	9.81	
I4		40.1	5.9	9.79	
Y1	Reference flax	Total length: 340	31.3	7.3	11.35
Y2		Free length: 290	31.7	7.3	11.45
Y3		Root length: 50	30.97	7.2	11.28
Y4			31.6	7.26	11.47
Z1	Reference carbon	Total length: 580	42.8	5.78	9.62
Z3		Free length: 490	43	5.76	9.62
Z4		Root length: 90	42	5.72	9.62



3 Theory

Natural frequencies for a cantilever beam can be calculated from equation (1):

$$f_n = \frac{k_n^2}{2\pi L^2} \left(\frac{EI}{\rho A} \right)^{1/2} \quad (1)$$

where,

E: equelent modulus of elasticity

I: second moment of area

ρ : density

A: cross-section area

L: beam free length

The subscript n refers to the mode number and using the eigenvalue solution, the first three modes can be calculated are:

$$k_1 = 1.875, k_2 = 4.694, k_3 = 7.855$$

Using classical laminate theory (CLT) the effective Young's modulus of the laminate, E_x , can be calculated as equation (2):

$$E_x = \frac{(A_{11}A_{22} - A_{12}^2)}{tA_{22}} \quad (2)$$

where, the components of A_{ij} in equation (2) can be calculate from :

$$A_{ij} = \int_{-t/2}^{t/2} (\bar{Q}_{ij})_k dz = \sum_{k=1}^n (\bar{Q}_{ij})_k (z_k - z_k) \quad (3)$$

where, the \bar{Q}_{ij} are the components of the transformed lamina stiffness matrix. The components of lamina stifness matrix Q_{ij} can be calculated using the material properties of each lamina as equation (4):

$$Q_{11} = \frac{E_1}{1 - \nu_{12}\nu_{21}} \quad (4)$$



$$Q_{11} = \frac{\nu_{12}E_1}{1 - \nu_{12}\nu_{21}}$$

$$Q_{11} = \frac{E_2}{1 - \nu_{12}\nu_{21}}$$

$$Q_{66} = G_{12}$$

For analytical results, the effective Young modulus for each specimen is calculated from the provided material properties. Then, knowing other properties and parameters such as density and specimen dimensions, the natural frequencies in first three modes of vibration can be calculated and compared to experimental results. The lamina properties provided by Kairos are presented in Table 3.

Table 3. properties of individual lamina

Material	E ₁ (GPa)	E ₂ (GPa)	ν ₁₂	Thickness (mm)	C ₅₅ (GPa)	Density (Kg/m ³)
UD Carbone (300g)	112.22	5.54	0.352	0.357	5.321	1469.20
UD Flax (200g)	19.96	4.42	0.320	0.360	2.470	1298.80
UD FlaxTape (110g)	26.25	4.42	0.320	0.194	2.138	1298.80
UD FlaxTape (70g)	26.25	4.42	0.320	0.124	2.138	1298.80
FLAX équilibré	12.19	12.19	0.116	0.541	2.470	1298.80
FLAX +/- 45°	7.27	7.27	0.473	0.541	5.463	1298.80

The dynamical properties corresponding to the 2nd resonance peak were determined by using 3-dB bandwidth (cut off frequency) method also known as the half power bandwidth method, as shown in Figure 4. In a FRF, the damping is proportional to the width of the resonant peak about the peak's center frequency. The damping factor (Q_n) is found by the equation (5):

$$Q_n = f_0 / (f_2 - f_1) \quad (5)$$

where:

f₀ = frequency of resonant peak in Hertz



f_2 = frequency value, in Hertz, 3 dB down from peak value, higher than f_0

f_1 = frequency value, in Hertz, 3 dB down from peak value, lower than f_0

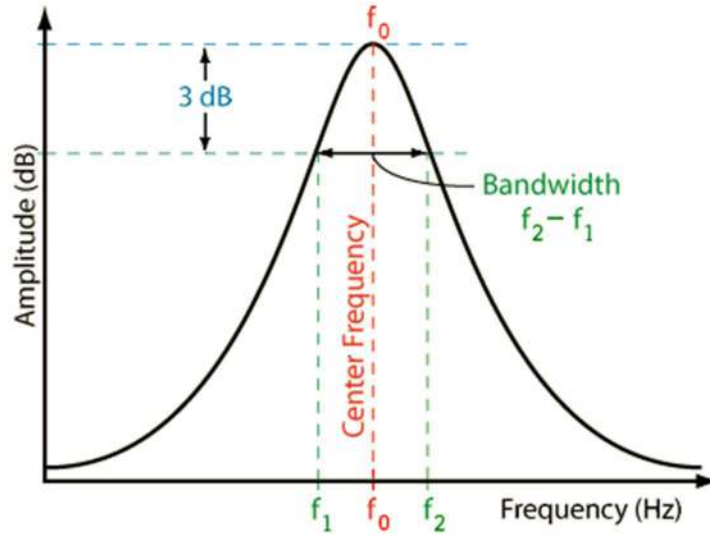


Figure 4. The 3 dB method diagram for calculating the damping factor Q

The relationship between damping factor (Q), damping ratio (ζ), and loss factor (η) is given in equation (6):

$$\eta_n = \frac{1}{Q_n} = 2 \cdot \zeta_n = \frac{\Delta f_{3dB}}{f_n} \quad (6)$$

where n=mode number, the half-power points are used to determine the damping ratio.



4 Results and Discussion

To ensure the accuracy and sensitivity of the sensors, the accelerometers were calibrated before conducting the experiments.

4.1 Calibration results and Input parameters

The out puts for calibration of each sensor and the input parameters are presented as follows:

Channel 1:

==== Measurement =====

Fspan : 240.0 Hz
 Same as Test : Off
 Lines : 800
 Number of Averages : 10
 Tolerance : 10.00%
 Freq Mode : Value

==== Calibrator =====

Number of Cal Chans : 1
 Freq : 159.2 Hz
 Cal Level : 1.000 g (RMS)

==== Channels =====

Ch#	EU	Ref (mV/EU)	Cal (mV/EU)	%Chg
1	g	500.3	532.8	6.49

Channel 2:

==== Measurement =====

Fspan : 240.0 Hz
 Same as Test : Off
 Lines : 800
 Number of Averages : 10
 Tolerance : 10.00%
 Freq Mode : Value

==== Calibrator =====

Number of Cal Chans : 1
 Freq : 159.2 Hz
 Cal Level : 1.000 g (RMS)

==== Channels =====

Ch#	EU	Ref (mV/EU)	Cal (mV/EU)	%Chg
2	g	482.1	519.5	7.76



Input Channels

C	Nam	Couplin	Range(eu	mV/e	e	Seria	Pt/Di	Windo
h	e	g)	u	u	l	r	w
1	I1	ICP	18.77	532.8	g	N/A	0:-Z	Flattop
2	I2	ICP	19.25	519.5	g	N/A	0:-Z	Flattop

4.2 Aluminum alloy beam as the reference material: Case 1

The experiment was conducted on the aluminium alloy beam with both the accelerometers of type B&K accelerometer 4507 (Figure 5). The accelerometer on the specimen were placed on the tip of the beam to measure the dynamic response of the beam. The vibration signal was swept from 10 to 1000 Hz with 2000 data points (linear distribution). The transfer function is presented in Figure 6. Following the full-range scan, in order to measure the resonance frequencies more accurately, several scans were conducted around range of each resonance frequency with 200 data points. The Young’s modulus of the aluminium alloy is calculated according to ASTM E756 and presented in Table 4.

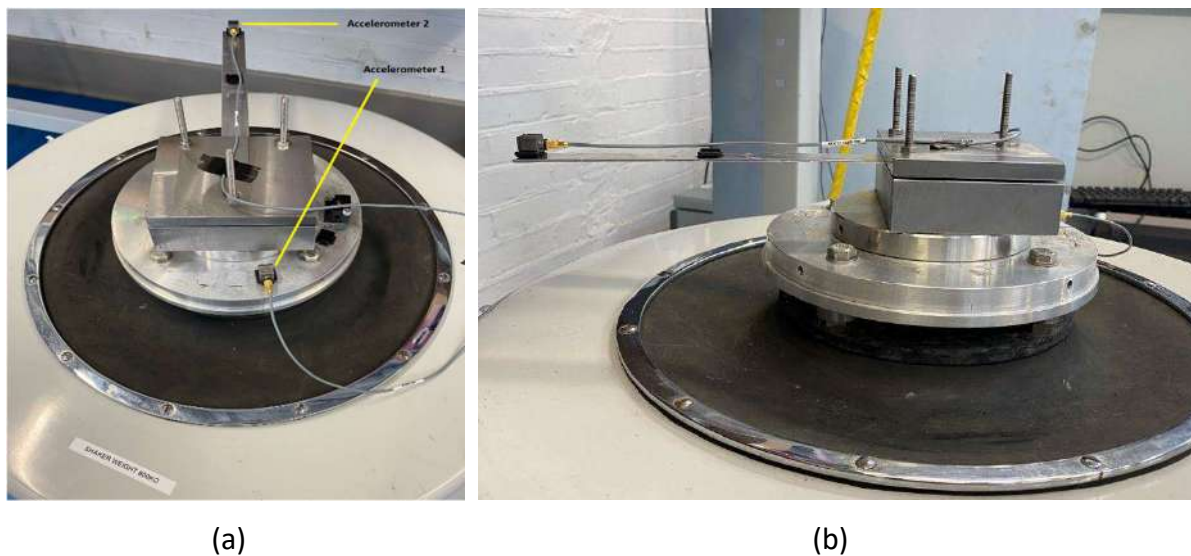


Figure 5. Experimental setup for aluminium alloy beam with B&K accelerometer type 4507 (a) top view; (b) side view

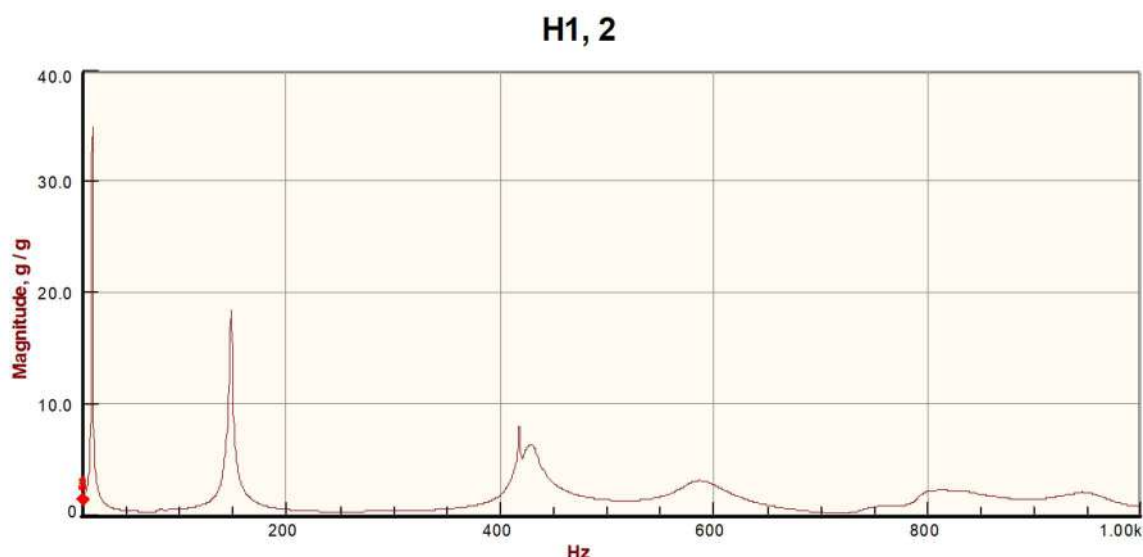
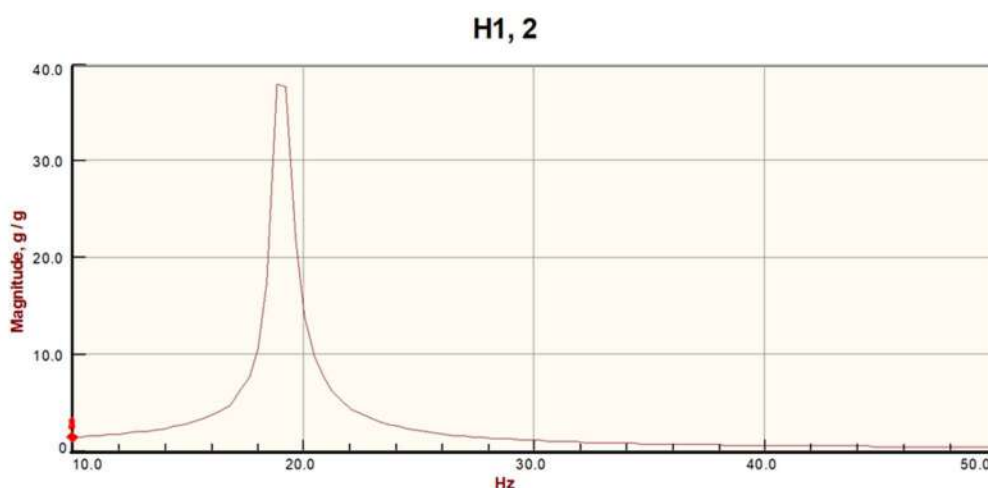


Figure 6. Transfer function for swept sine signal (10 Hz to 1000 Hz)

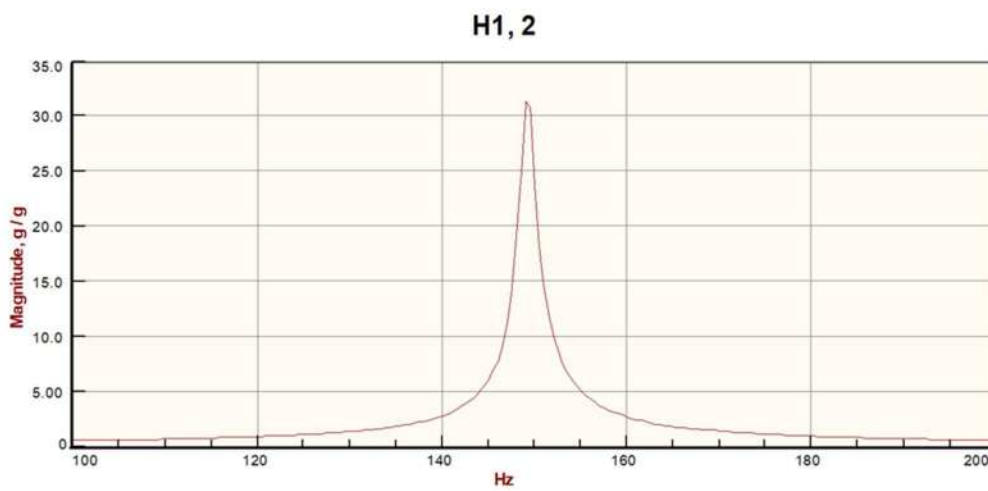
It is observed from Figure 6 that the resonance frequencies occur at 19.4 Hz, 149 Hz and 429 Hz.

In order to measure the resonance frequencies more accurately, several scans were conducted for the following frequency range: 10-50 Hz; 100-200 Hz, 400-500 Hz

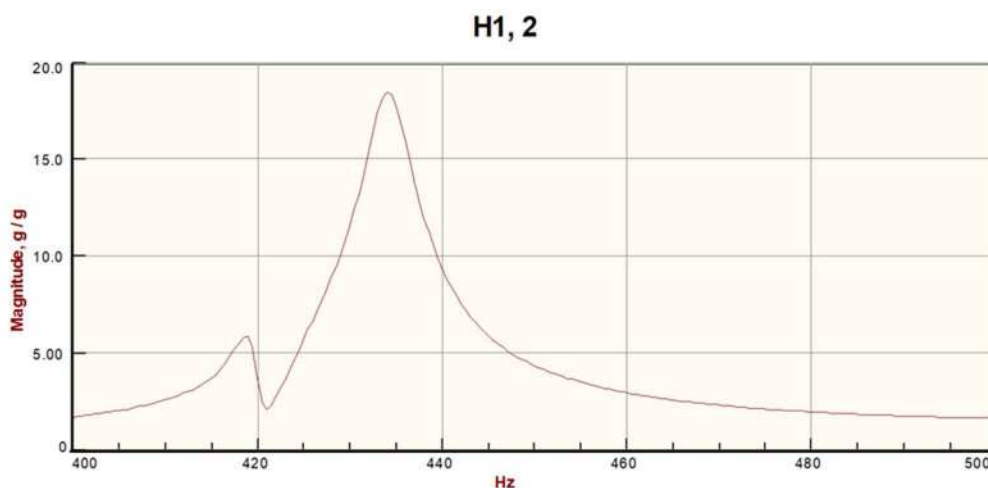
The transfer functions for the 10-50 Hz, 100-200 Hz, and 400-500 Hz frequency ranges are presented in Figure 7(a)-6(c) respectively. The resonance frequencies are identified at 18.9 Hz, 149 Hz and 434 Hz respectively.



(a)



(b)



(c)

Figure 7. Transfer function for swept sine signal (a) 10 Hz to 50 Hz; (b) 100 Hz to 200 Hz; (c) 400 Hz to 500 Hz

It is observed from Table 4 that the Young's modulus of the aluminium alloy deviate by 33% than that of the theoretical value. The probable reason of the error was assumed to be the mass of the accelerometer. In order to minimize the effect of the mass of the accelerometer, a lighter accelerometer (B&K accelerometer type 4517) was used.



Table 4. Calculation of Young’s modulus of aluminium alloy using B&K accelerometer type 4507

ASTM E756 - Aluminum sample									
	unit	values				average	standard dev.	average (n>1)	standard dev. (n>1)
rho	kg/m3	2700	-	-	-	-	-		
l	m	0,2	-	-	-	-	-		
H	m	1,45E-03	-	-	-	-	-		
fn	Hz	26,075	141,67	434,3	866,75	-	-		
Cn	-	0,55959	3,5069	9,8194	19,242	-	-		
E	MPa	53535	40238	48232	50028	48008	4875	46166	4255
E theory	MPa	69000	69000	69000	69000	69000	nc		
(E-Eth)/Eth	%	-22%	-42%	-30%	-27%	-30%		-33%	6%
η (-3dB meth)	%	2,5%	1,6%	1,5%	1,3%	1,7%	0,5%	1,4%	0,1%



4.3 Aluminum alloy beam as the reference material: Case 2

The experiment for case 2 was conducted on the same aluminium alloy beam used for case 1. B&K accelerometer type 4517 accelerometer was attached on the tip of the cantilever beam to measure the dynamic response of the beam and B&K accelerometer type 4507 was mounted on the shaker to control the acceleration of the shaker as shown in Figure 8. The vibration signal was swept from 10 to 1200 Hz with 500 data points (linear distribution) and the transfer function is presented in Figure 9.

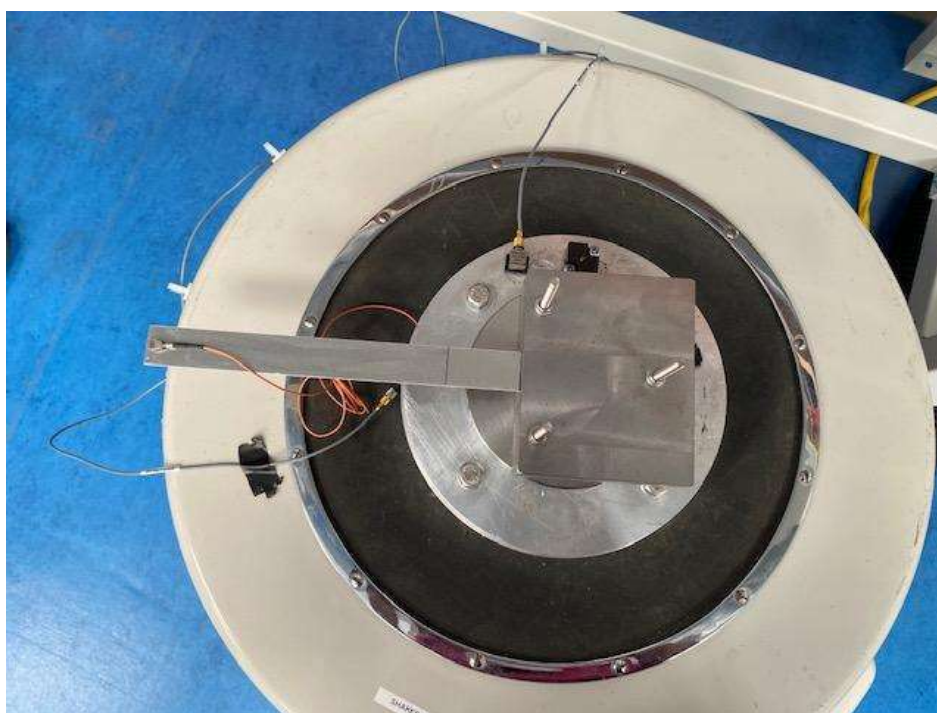


Figure 8. Experimental setup for aluminium alloy beam with B&K accelerometer type 4517 at the tip

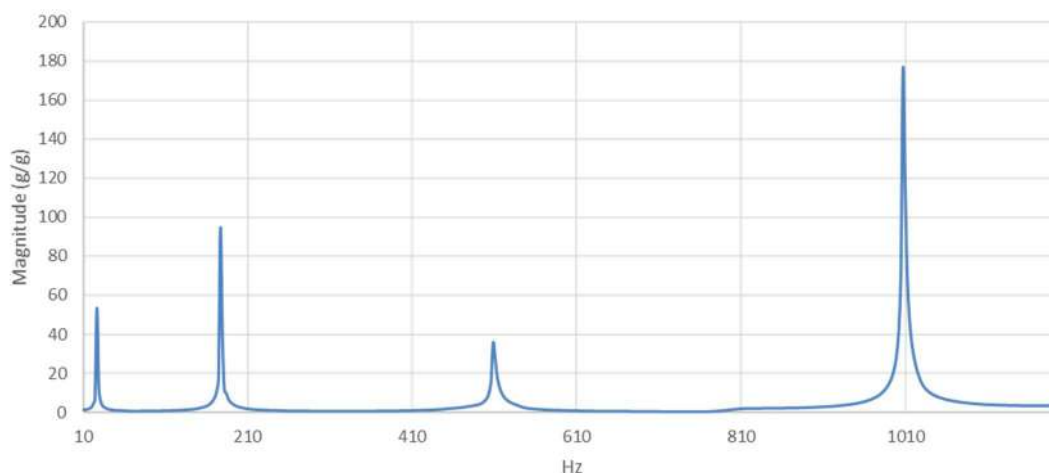


Figure 9. Transfer function for swept sine signal (10 Hz to 1200 Hz)



The resonance frequencies are identified at 26.7 Hz, 177 Hz, 508 Hz and 1010 Hz as shown in Figure 9.

Following the full-range scan, in order to measure the natural frequencies and damping ratios more accurately, three scans were conducted around range of each natural frequency. The following frequency ranges were considered for the swept sine signal and the corresponding transfer functions are presented in Figure 10(a)-9(d) respectively:

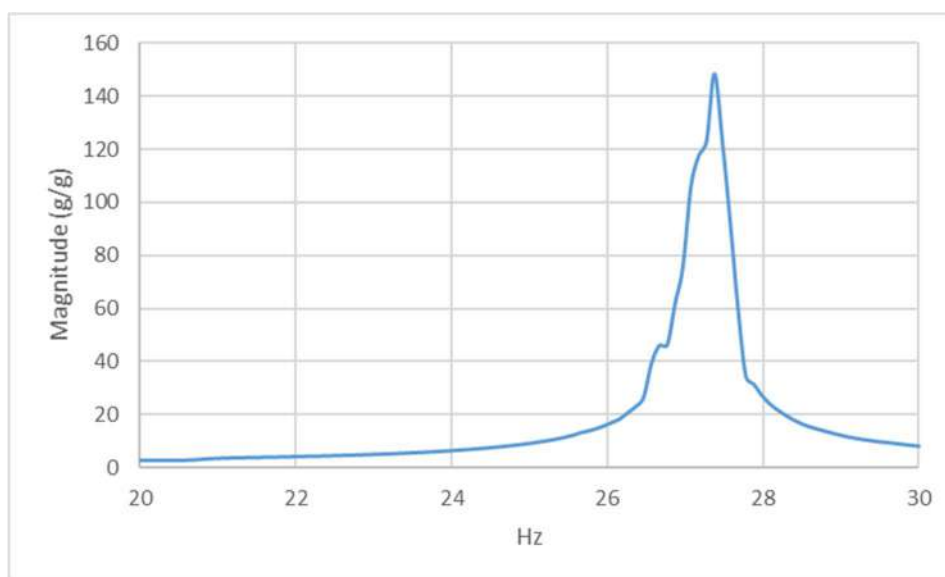
20-30 Hz with 100 linear data points

165-185 Hz with 100 linear data points

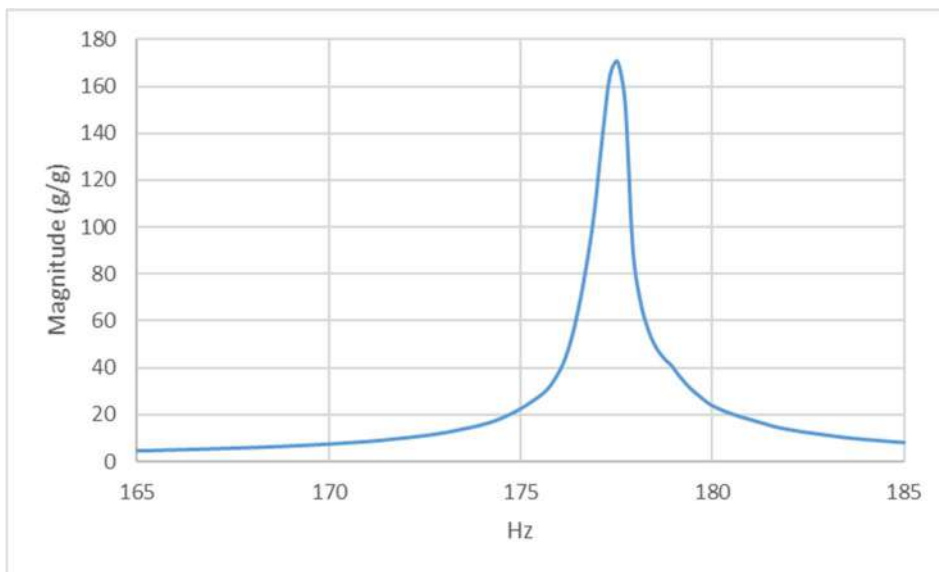
500-520 Hz with 100 linear data points

990-1020 Hz with 100 linear data points

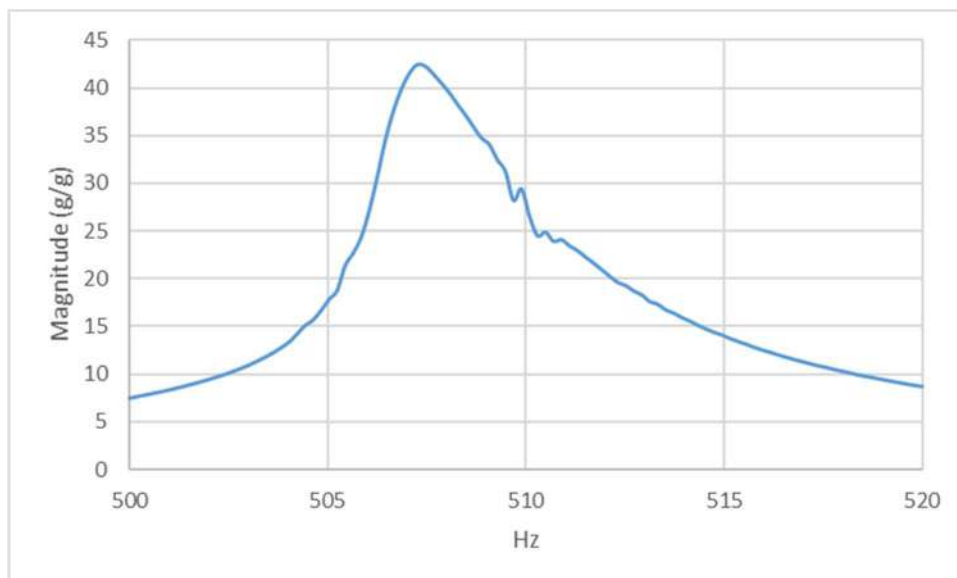
The resonance frequencies are identified at 27.4 Hz, 178 Hz, 507 Hz and 1010 Hz respectively.



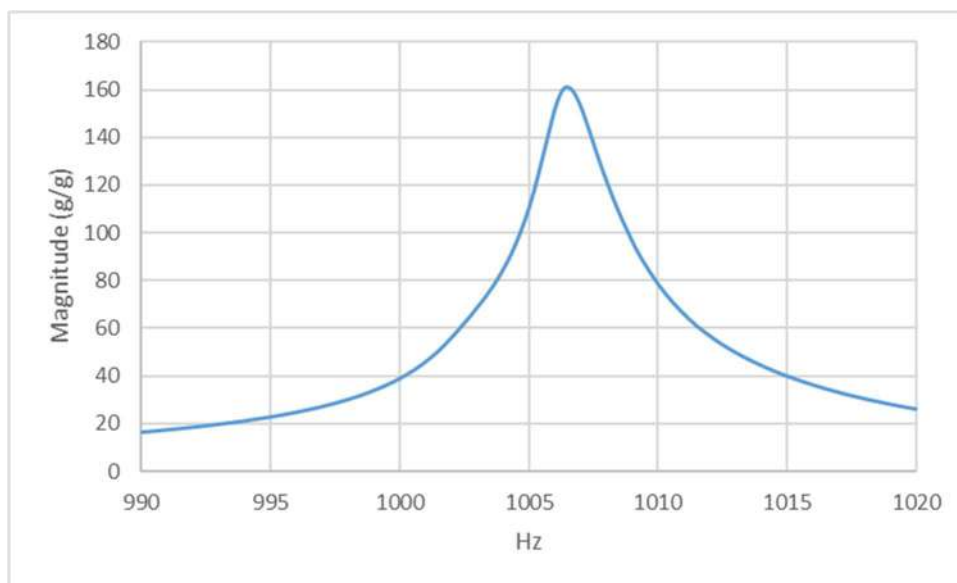
(a)



(b)



(c)



(d)

Figure 10. Transfer function for swept sine signal (a) 20 Hz to 30 Hz; (b) 165 Hz to 185 Hz; (c) 500 Hz to 520 Hz; (d) 990 Hz to 1020 Hz

The calculation of Young's modulus is presented in Table 5. The resonance frequencies obtained from numerical modelling is presented in Table 6 and compared with the experimental values. It is observed from Table 5 that the Young's modulus of the aluminium alloy deviate by 1% from the theoretical value. The improvement in the calculation of Young's modulus signifies the effect of the mass of the accelerometer on the experimental outcome. It is evident that the added mass from the accelerometer can be neglected for the lighter accelerometer.

Table 6 clearly demonstrates that the experimental resonance frequencies agree well with resonance frequencies obtained from numerical modelling with an average deviation of 0.5%.



Table 5. Calculation of Young's modulus of aluminium alloy using B&K accelerometer type 4517

ASTM E756 - Aluminum sample									
Parameter	unit	values				average	std	average (n>1)	std (n>1)
Rho (ρ)	kg/m ³	2887	-	-	-	-	-		
l	m	0,2	-	-	-	-	-		
H	m	1,45E-03	-	-	-	-	-		
fn	Hz	27,4	177,5	507,3	1006,5	-	-		
Cn	-	0,55959	3,5069	9,8194	19,242	-	-		
E	MPa	63093	67525	70373	72132	68281	3417	70010	1898
E theory	MPa	69000	69000	69000	69000	69000			
(E-Eth)/Eth	%	-9%	-2%	2%	5%	-1.0%		1.5%	3%
η	%	1,7%	0,5%	0,7%	0,3%	0,8%	0,5%	0,5%	0,1%
η theory*	%	0,197	0,079	0,057	-				

Table 6. Numerical result for the aluminium alloy cantilever beam

Frequency FEA (Hz)	27,9	173,5	502,4	1018,2
Frequency shaker (Hz)	27,4	177,5	507,3	1006,5
diff with shaker (%)	1,8%	-2,3%	-1,0%	0,0
FRF (dB)	57,0	75,6	70,7	40,0
Damping factor (Q)	1450	5115	4963	-
Loss factor FEA (eta)	0,07%	0,02%	0,02%	-
Loss factor shaker (eta)	1,70%	0,47%	0,65%	0,32%
diff with shaker (%)	-96%	-96%	-97%	-
Damping ratio (zeta)	0,03%	0,01%	0,01%	-



4.4 Aluminum alloy beam as the reference material: Case 3

This experiment was also conducted on the same aluminium alloy cantilever beam with the lighter accelerometer placed at 0.8l distance (160 mm) from the clamped end as shown in Figure 11. The vibration signal was swept from 10 to 1200 Hz with 600 data points (linear distribution) and the transfer function is presented in Figure 12.

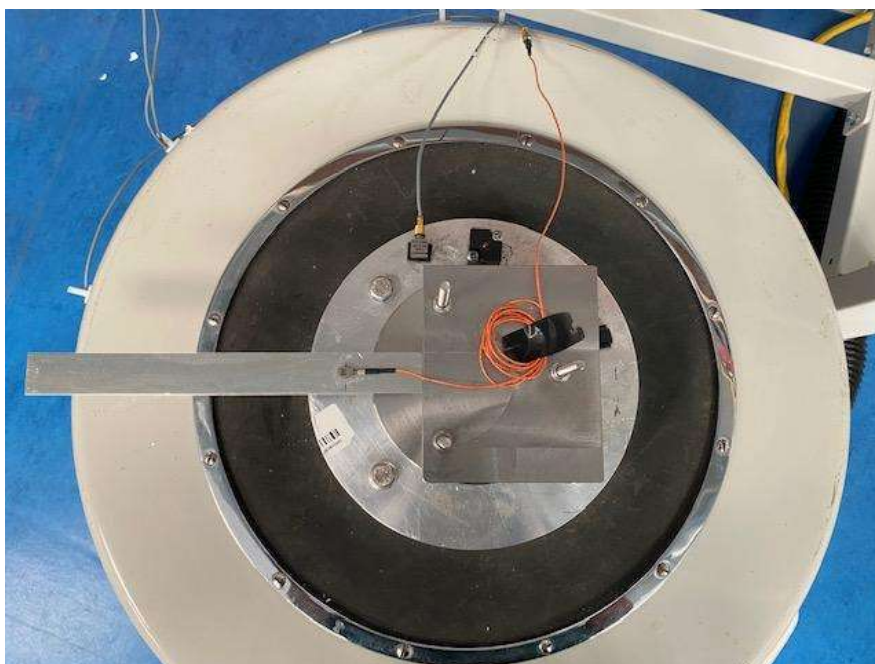


Figure 11. Experimental setup for aluminium alloy beam with B&K accelerometer type 4517 near the clamped end

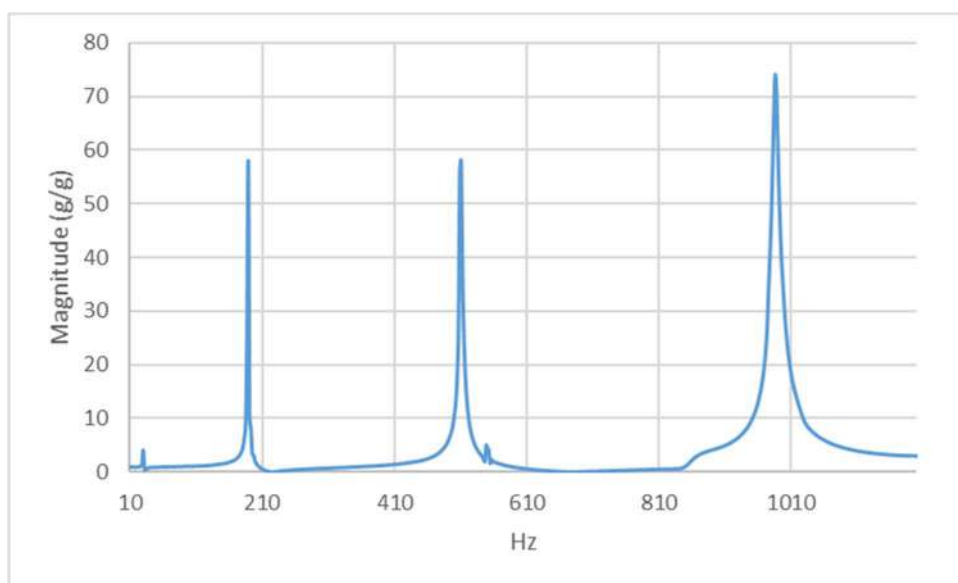


Figure 12. Transfer function for swept sine signal (10 Hz to 1200 Hz)



The resonance peaks are observed at 29.9 Hz, 189 Hz, 511 Hz and 985 Hz.

In order to measure the resonance frequencies more accurately, several scans were conducted around range of each resonance frequency for the following frequency range:

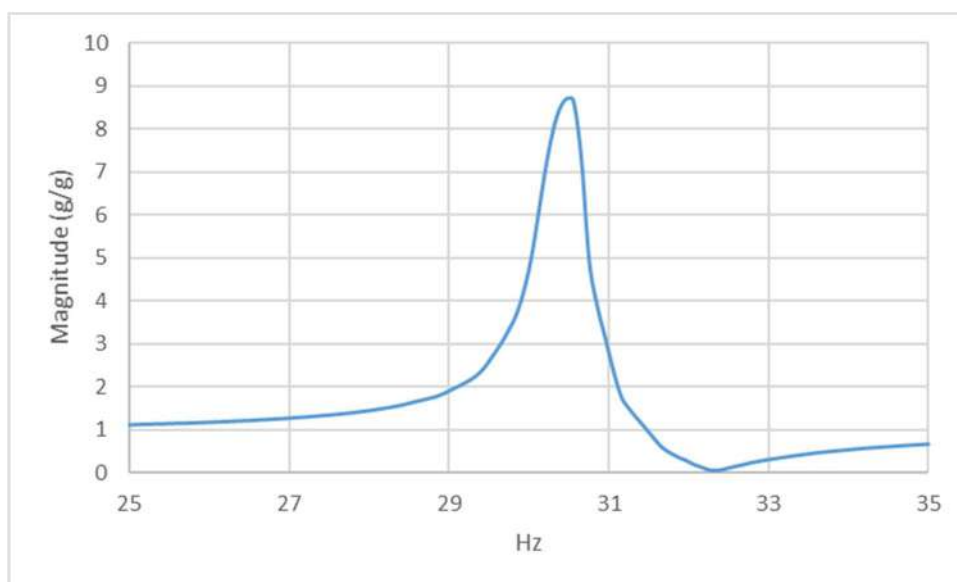
25-35 Hz with 100 linear data points

175-195 Hz with 100 linear data points

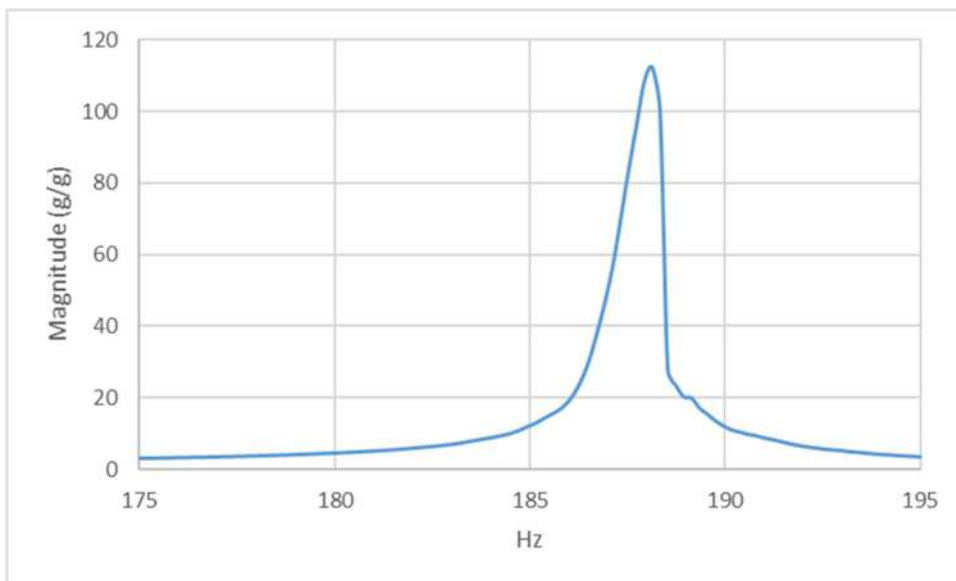
495-520 Hz with 125 linear data points

950-1010 Hz with 200 linear data points

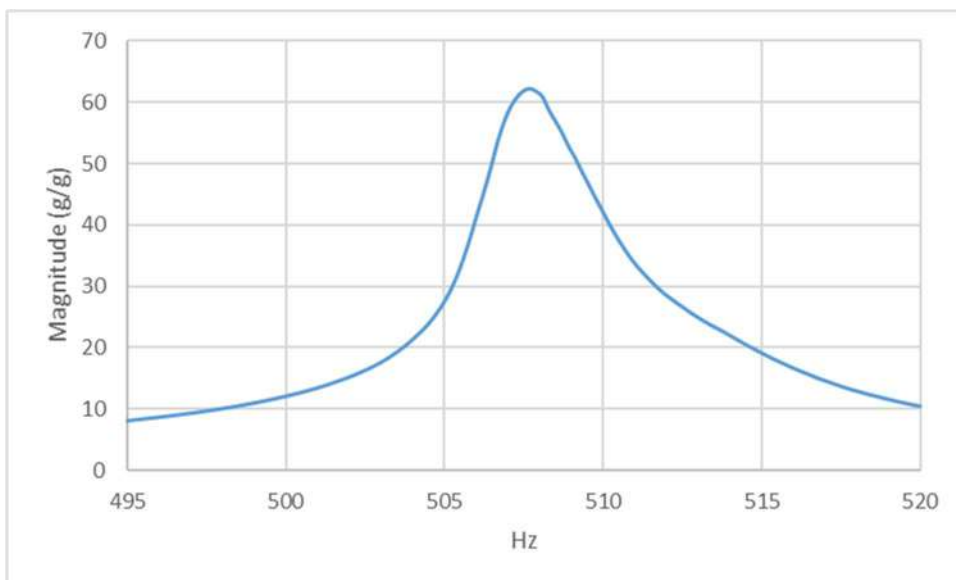
The corresponding transfer functions are presented in Figure 13(a)-12(d) respectively. The resonance frequencies are identified at 30.6 Hz, 188 Hz, 508 Hz and 984 Hz.



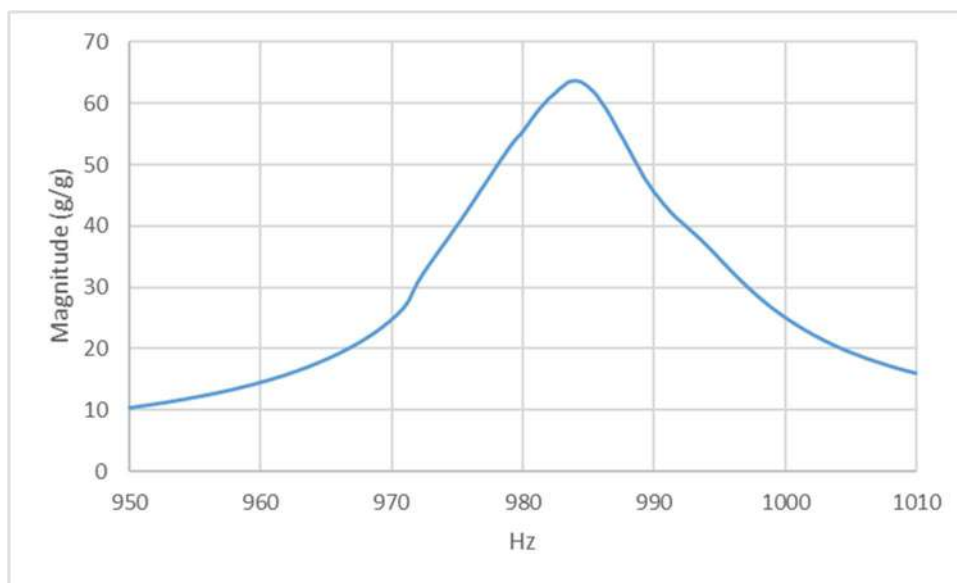
(a)



(b)



(c)



(d)

Figure 13. Transfer function for swept sine signal (a) 25 Hz to 35 Hz; (b) 175 Hz to 195 Hz; (c) 495 Hz to 520 Hz; (d) 950 Hz to 1010 Hz

4.5 Test on flax/carbon hybrid epoxy beam

This test was conducted on the hybrid flax/carbon fibre reinforced composite beam. The laminate has flax fibre on the outer layers and carbon fibre in the inner layers. The damping experiment was conducted in accordance with ASTM E756 using an electrodynamic shaker. The specimen (as mentioned in Table 1) was clamped to the shaker using two steel blocks mounted on the shaker as shown in Figure 14. This effectively made the specimen into a cantilever beam; the specimen was free to vibrate naturally at one end and locked completely at the other end. A sensor (B&K accelerometer type 4517) was attached to the specimen at 0.8l distance (144 mm) from the clamped end to measure the dynamic response of the beam. Another sensor (B&K accelerometer type 4507) was mounted to the shaker to control the excitation of the shaker.

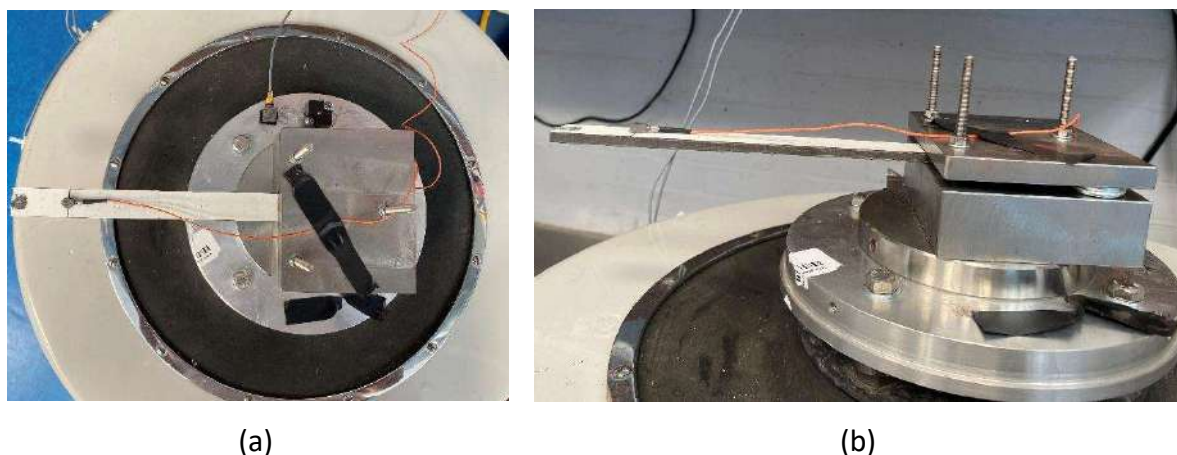


Figure 14. Experimental setup for flax/carbom hybrid epoxy beam (a) top view; (b) side view

The vibration signal was swept from 100 Hz to 3000 Hz with 1500 linear data points. The transfer function is presented in Figure 15. The resonance frequencies are identified at 135 Hz, 870 Hz, 986 Hz, and 2480 Hz.

To measure the resonance frequencies and damping ratios more accurately, several scans were conducted around range of each natural frequency for the following frequency range:

120-150 Hz with 300 data points with resonance frequency identified at 134 Hz

840-900 Hz with 300 data points with resonance frequency identified at 870 Hz

950-1030 Hz with 400 data points with resonance frequency identified at 986 Hz

2400-2560 Hz with 800 data points with resonance frequency identified at 2485 Hz

The transfer functions are presented in Figure 16(a)-15(d) respectively.

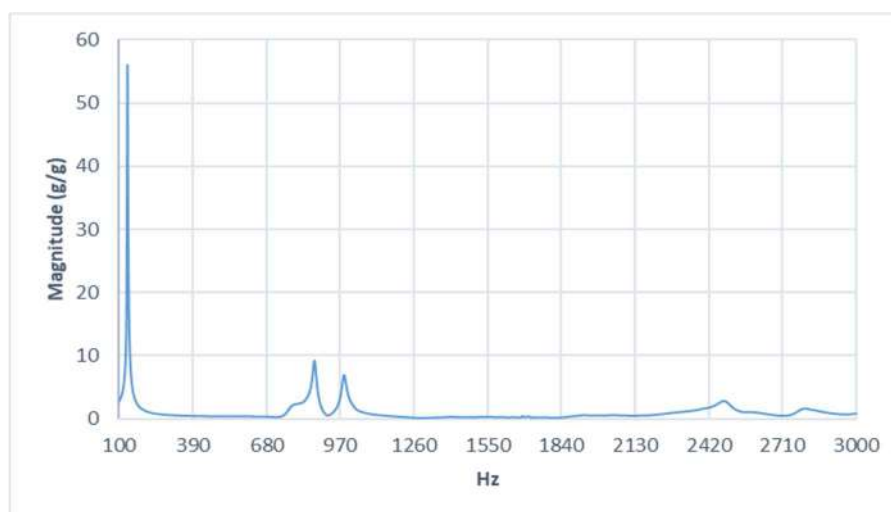
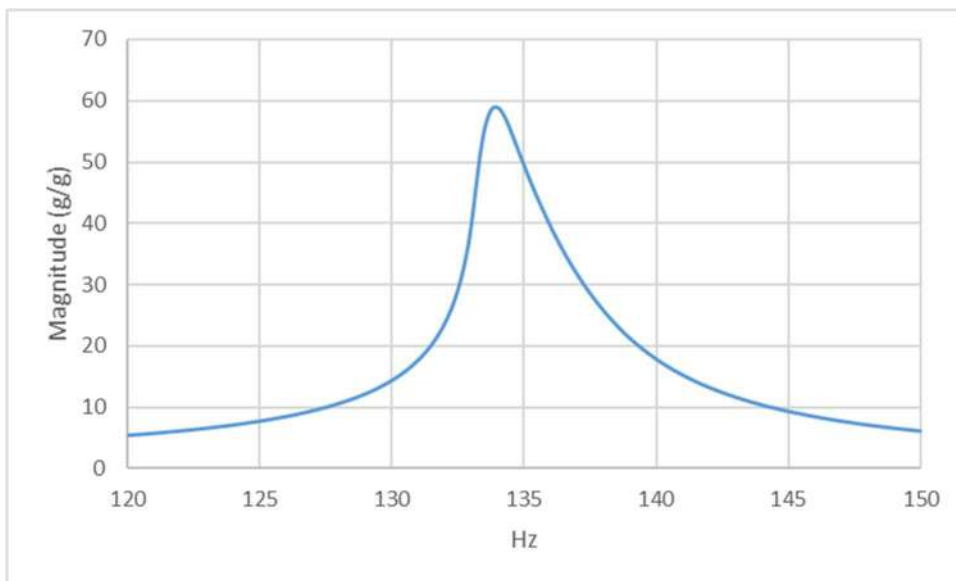
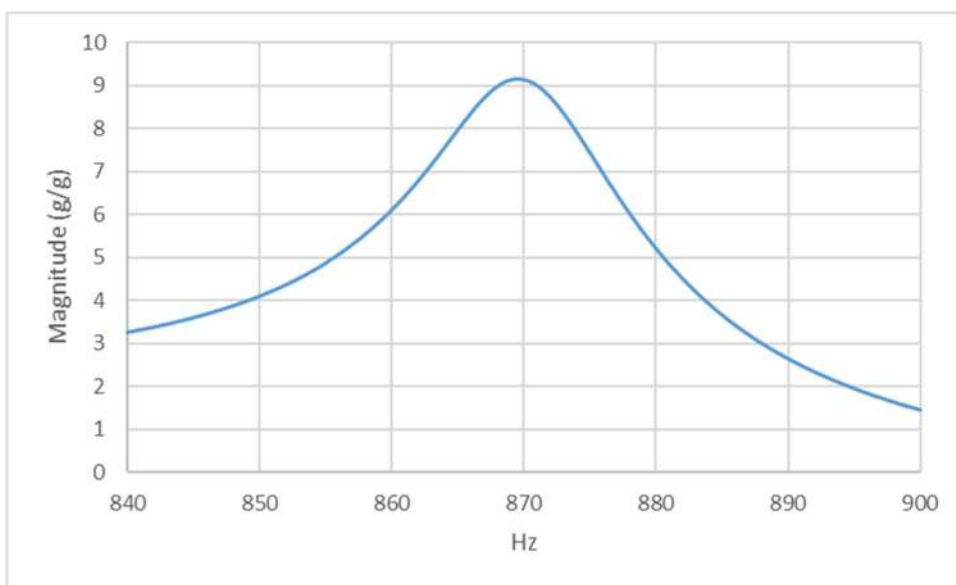


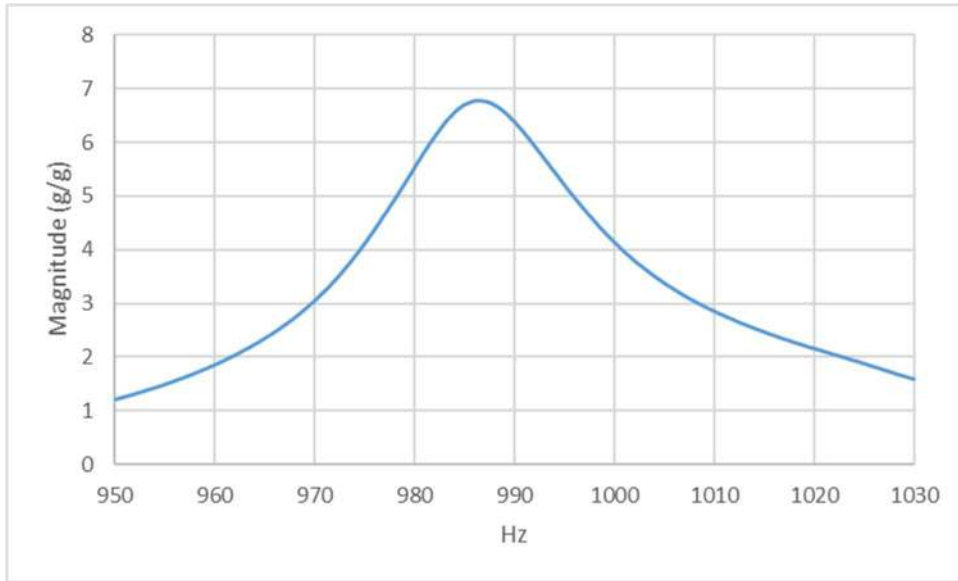
Figure 15. Transfer function for swept sine signal (100 Hz to 3000 Hz)



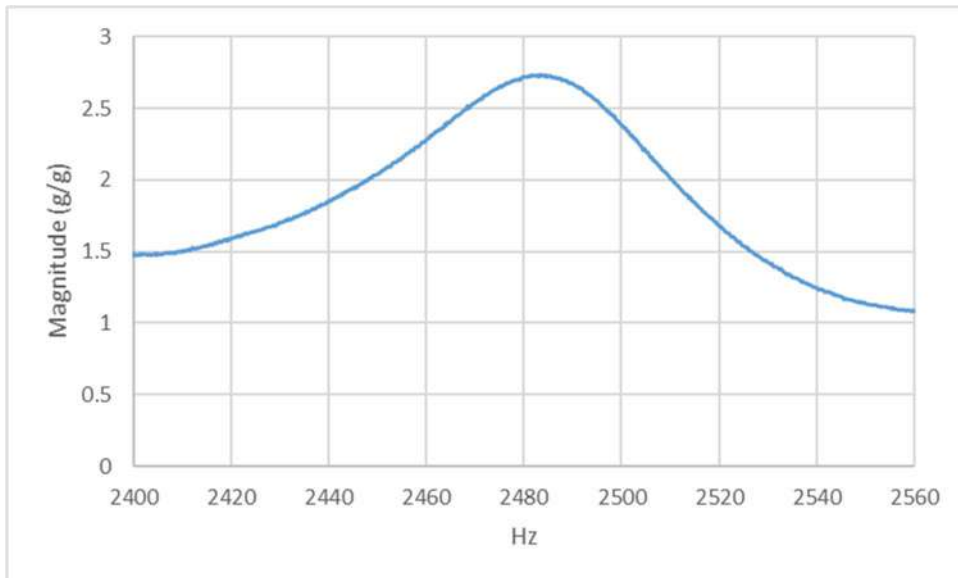
(a)



(b)



(c)



(d)

Figure 16. Transfer function for swept sine signal (a) 120 Hz to 150 Hz; (b) 840 Hz to 900 Hz; (c) 950 Hz to 1030 Hz; (d) 2400 Hz to 2560 Hz



4.6 Test on flax/epoxy composite beam 1: Case 1

This test was conducted on the flax/epoxy composite beam 1. The specimen (as described in Table 1) was clamped to the shaker using two steel blocks mounted on the shaker as shown in Figure 17. This effectively made the specimen into a cantilever beam; the specimen was free to vibrate naturally at one end and locked completely at the other end. A sensor (B&K accelerometer type 4517) was attached to the specimen at 0.8l distance (160 mm) from the clamped end to measure the dynamic response of the beam. Another sensor (B&K accelerometer type 4507) was mounted to the shaker to control the excitation of the shaker.

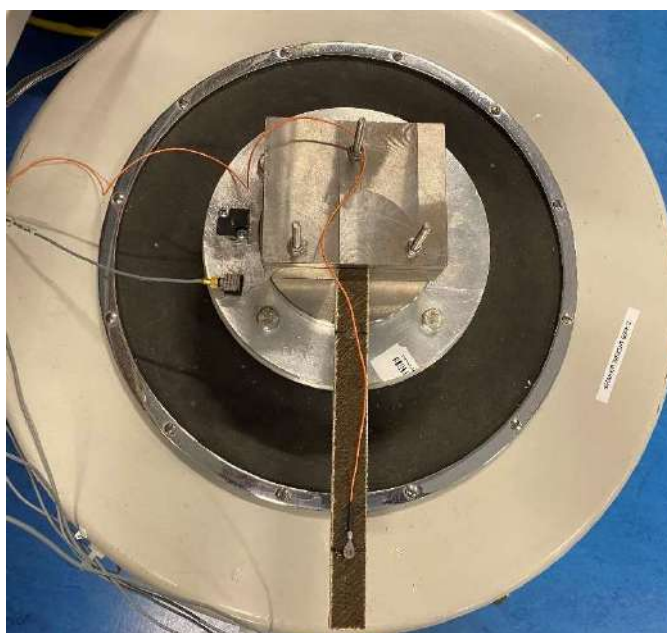


Figure 17. Experimental setup for flax/epoxy composite beam 1: Case 1

The vibration signal was swept from 10 to 1000 Hz with 500 data points (linear distribution). The transfer function is presented in Figure 18. The resonance frequencies are identified at 19.9 Hz, 137 Hz, 379 Hz, 722 Hz and 780 Hz. Following the full-range scan, in order to measure the resonance frequencies more accurately, several scans were conducted around range of each resonance frequency. The frequency ranges are as follows: 15-25 Hz (200 data points), 130-150 Hz (200 data points), 360-400 Hz (200 data points), 700-740 Hz (160 data points), and 750-830 Hz (320 data points) with resonance frequencies at 20.1 Hz, 138 Hz, 381 Hz, 726 Hz and 784 Hz respectively. The transfer functions are presented in Figure 19(a)-18(e).

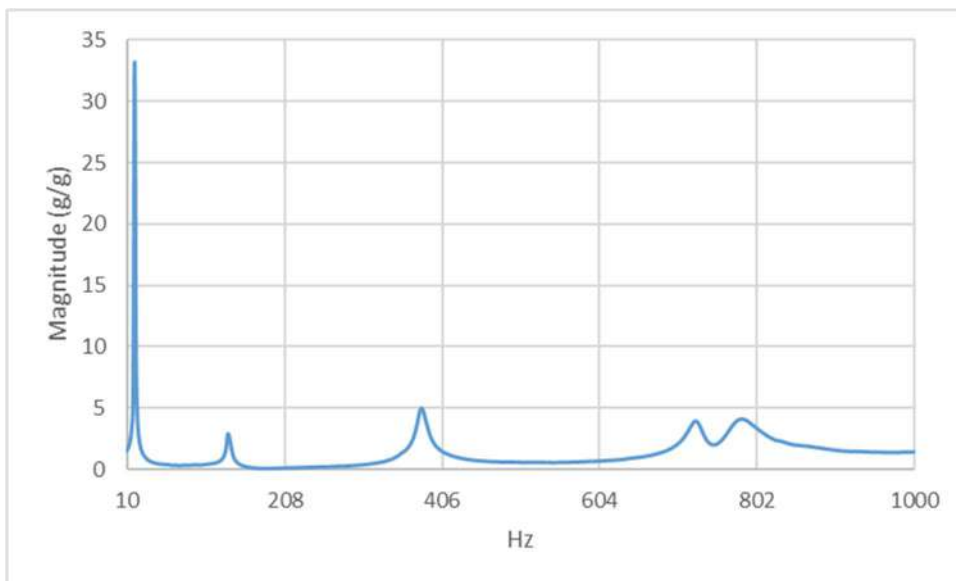
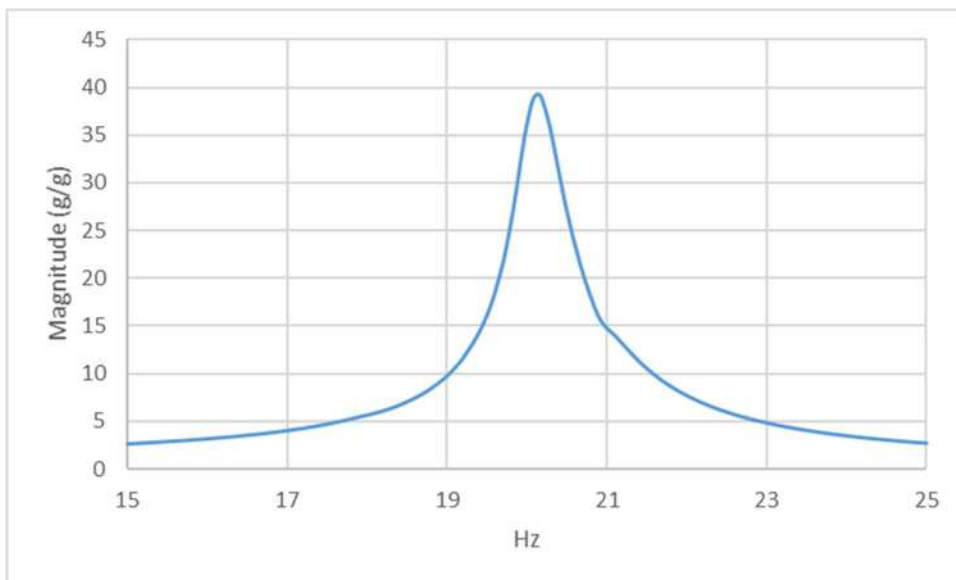
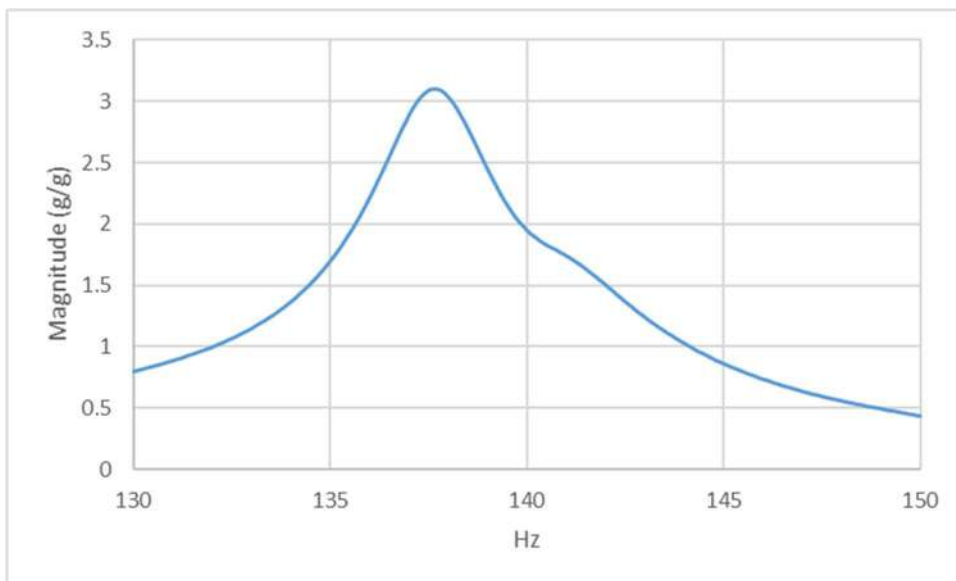


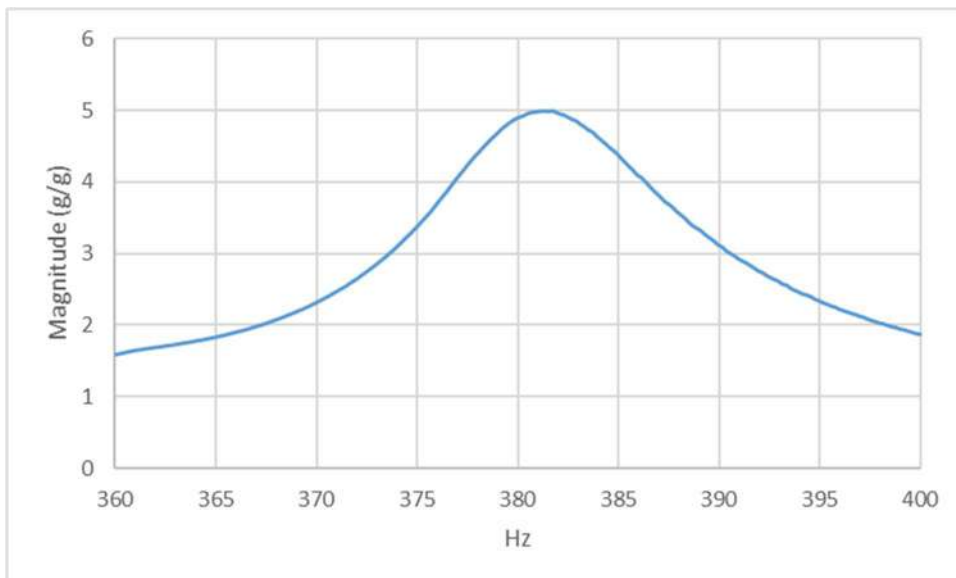
Figure 18. Transfer function for swept sine signal (10 Hz to 1000 Hz)



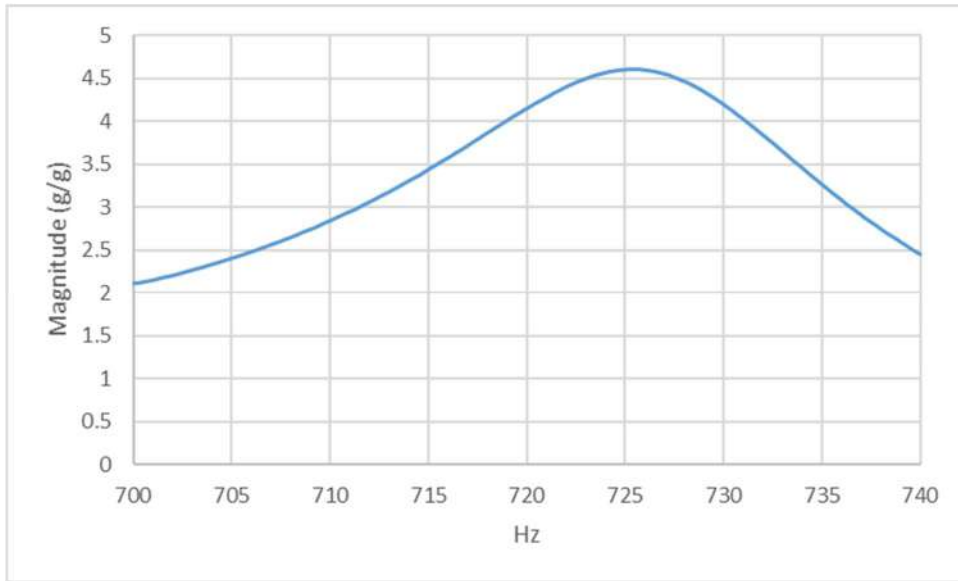
(a)



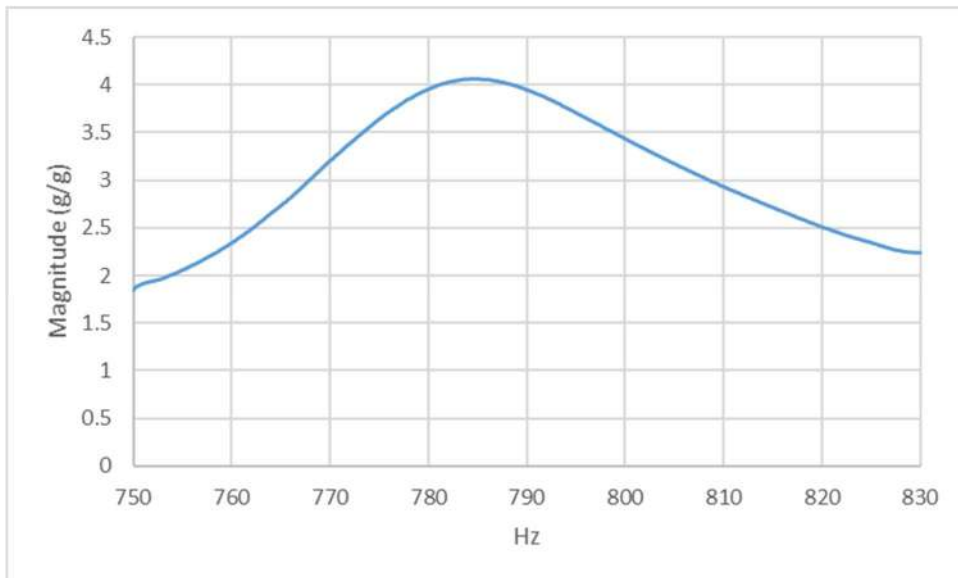
(b)



(c)



(d)



(e)

Figure 19. Transfer function for swept sine signal (a) 15 Hz to 25 Hz; (b) 130 Hz to 150 Hz; (c) 360 Hz to 400 Hz; (d) 700 Hz to 740 Hz; (e) 750 Hz to 830 Hz



4.7 Test on flax/epoxy composite beam 1: Case 2

This test was conducted on the flax/epoxy composite beam 1. The accelerometer was attached to the specimen at 0.2l distance (40 mm) from the clamped end to measure the dynamic response of the beam as shown in Figure 20. Another sensor was mounted to the shaker to control the excitation of the shaker.

The vibration signal was swept from 10 to 1000 Hz with 500 data points (linear distribution). The transfer function is presented in Figure 21. The resonance frequencies are identified at 21.9 Hz, 137 Hz, 375 Hz, 714 Hz and 790 Hz. Following the full-range scan, in order to measure the resonance frequencies more accurately, several scans were conducted around range of each resonance frequency. The frequency ranges are as follows: 16-26 Hz (200 data points), 130-150 Hz (200 data points), 360-390 Hz (150 data points), 680-750 Hz (280 data points), and 750-830 Hz (320 data points) with resonance frequencies at 21.9 Hz, 137 Hz, 376 Hz, 714 Hz and 788 Hz respectively. The transfer functions are presented in Figure 22(a)-21(e).

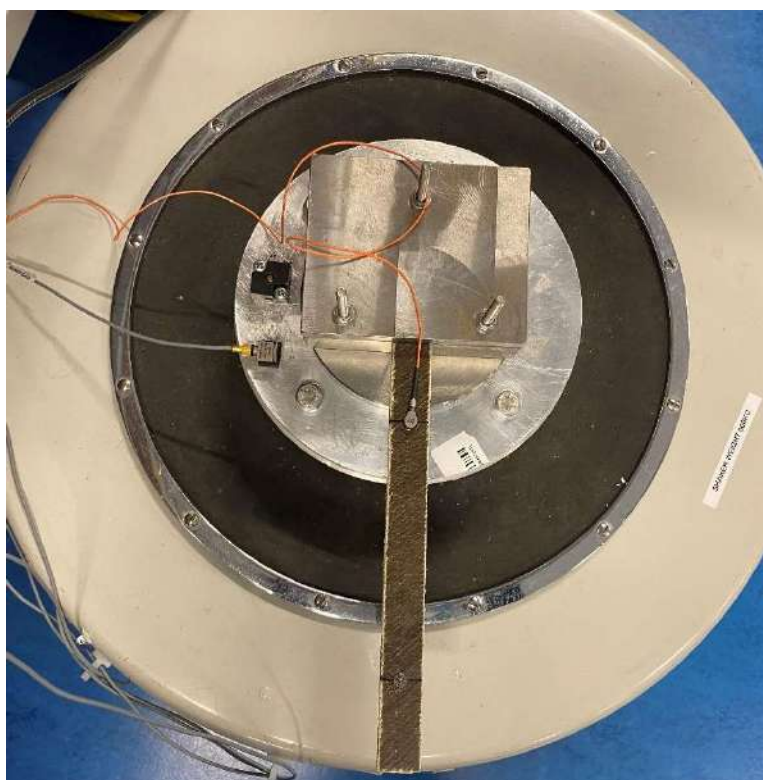


Figure 20. Experimental setup for flax/epoxy composite beam 1: Case 2

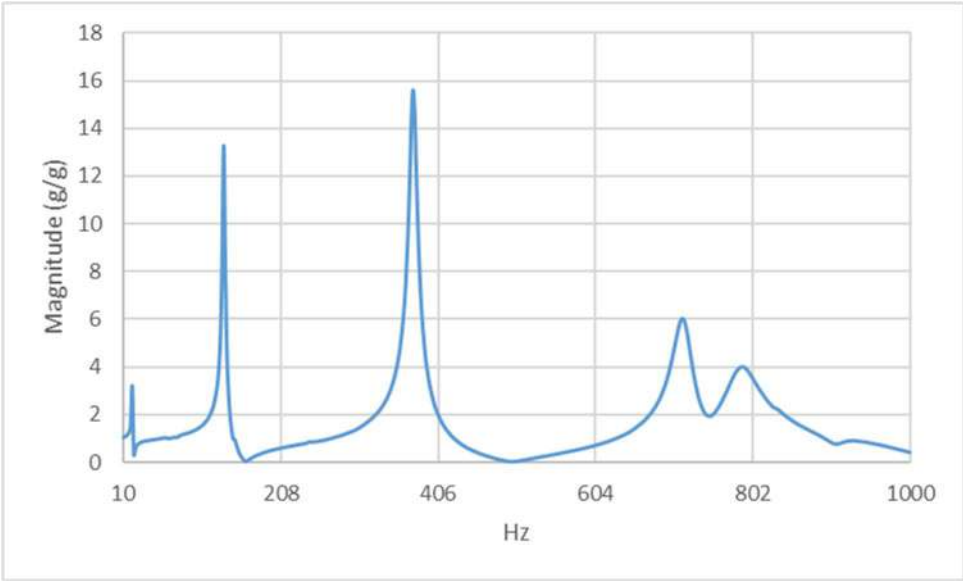
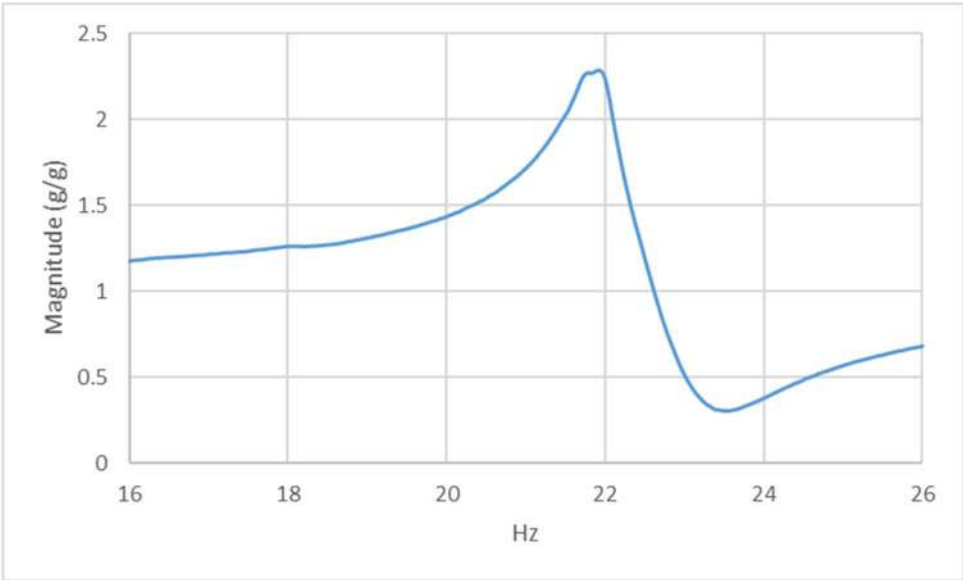
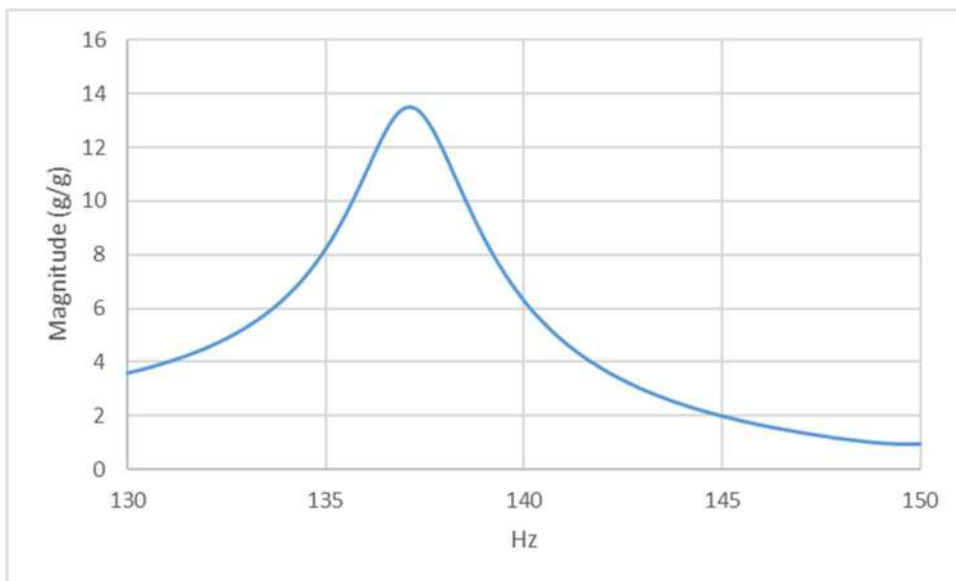


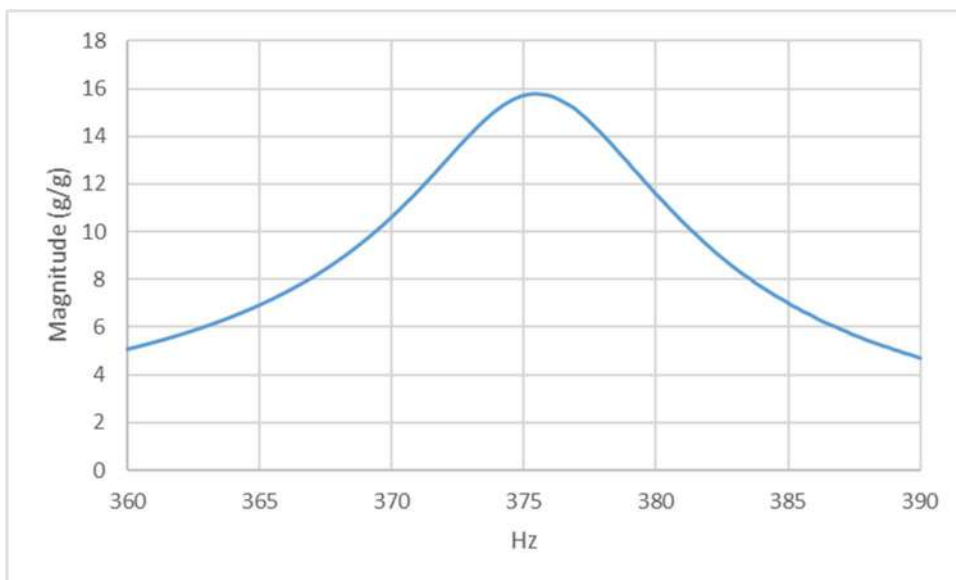
Figure 21. Transfer function for swept sine signal (10 Hz to 1000 Hz)



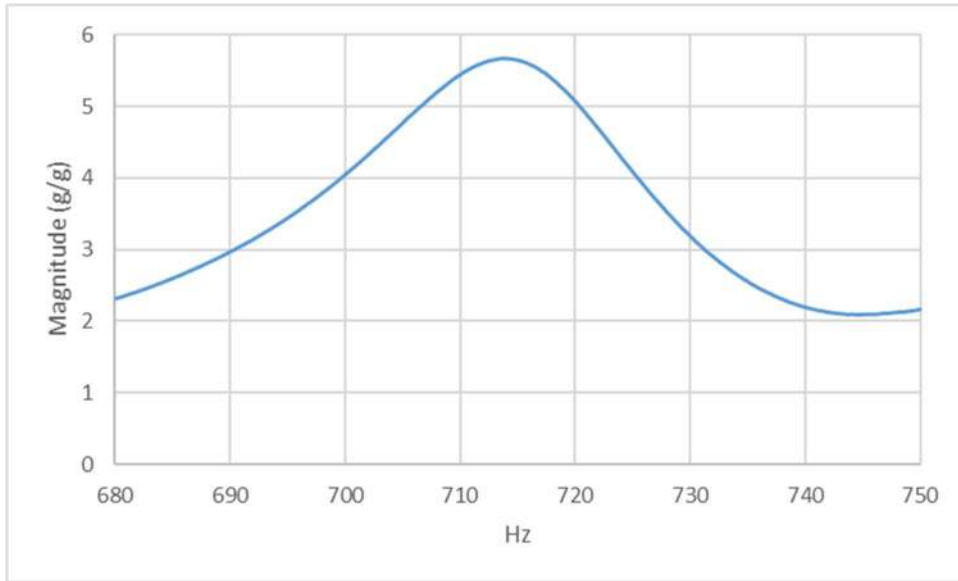
(a)



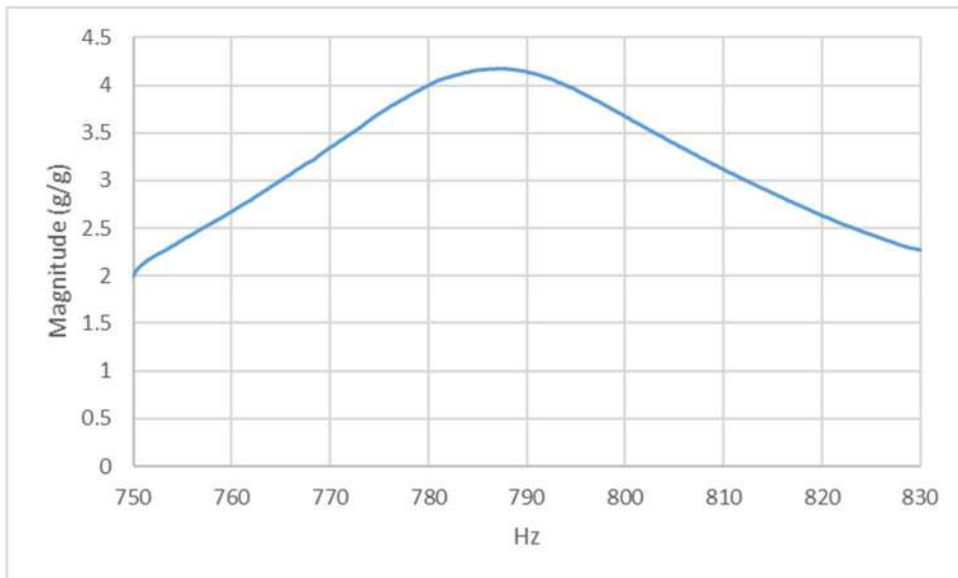
(b)



(c)



(d)



(e)

Figure 22. Transfer function for swept sine signal (a) 16 Hz to 26 Hz; (b) 130 Hz to 150 Hz; (c) 360 Hz to 390 Hz; (d) 680 Hz to 750 Hz; (e) 750 Hz to 830 Hz



The mode shapes obtained from FEM are presented in Figure 23.

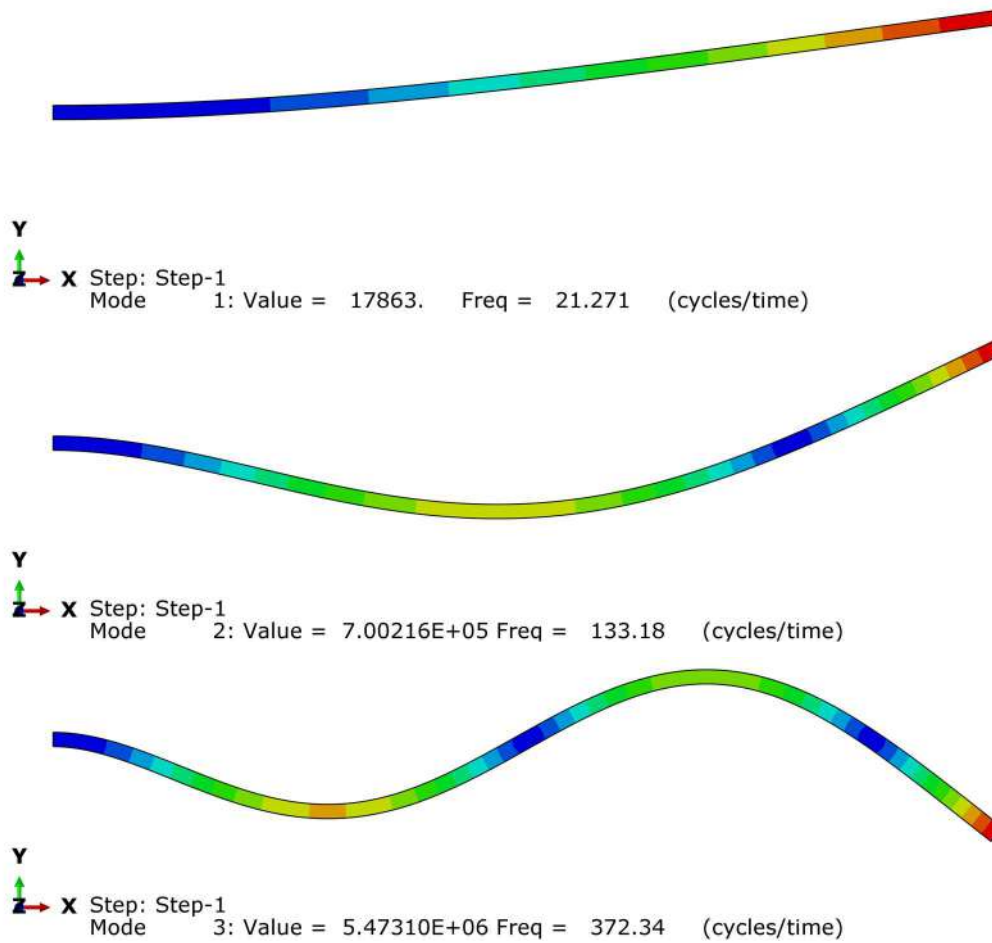


Figure 23. First three frequencies of vibration for flax/epoxy composite (beam 1) calculated by Abaqus FEM



4.8 Test on flax/epoxy composite beam 2: Case 1

This test was conducted on the flax/epoxy composite beam 2. The specimen (as mentioned in Table 1) was clamped to the shaker using two steel blocks mounted on the shaker as shown in Figure 24. This effectively made the specimen into a cantilever beam; the specimen was free to vibrate naturally at one end and locked completely at the other end. A sensor (B&K accelerometer type 4517) was attached to the specimen at 0.8l distance (93.6 mm) from the clamped end to measure the dynamic response of the beam. Another sensor (B&K accelerometer type 4507) was mounted to the shaker to control the excitation of the shaker.

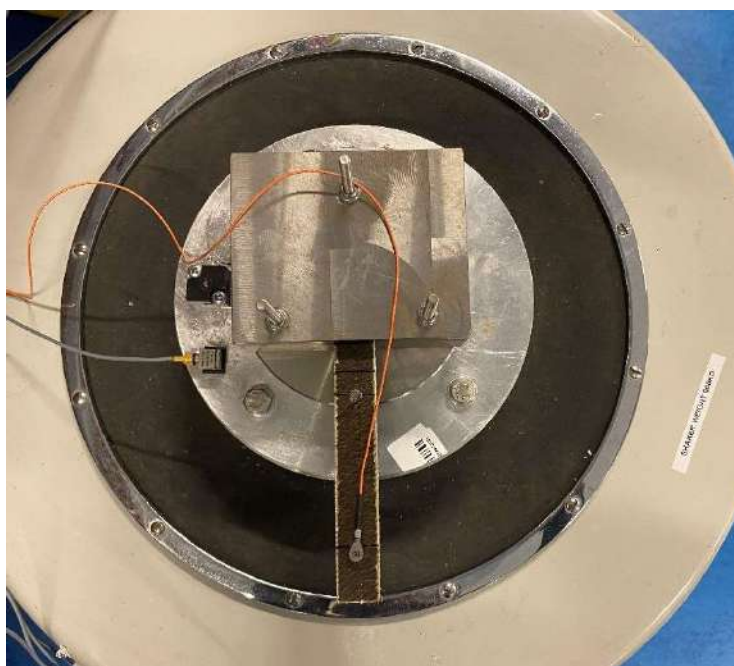


Figure 24. Experimental setup for flax/epoxy composite beam 2: Case 1

The vibration signal was swept from 10 to 1500 Hz with 750 data points (linear distribution). The transfer function is presented in Figure 25. The resonance frequencies are identified at 55.8 Hz, 1020 Hz and 1310 Hz. Following the full-range scan, in order to measure the resonance frequencies more accurately, several scans were conducted around range of each resonance frequency. The frequency ranges are as follows: 45-65 Hz (200 data points), 950-1090 Hz (500 data points), and 1240-1380 Hz (500 data points) with resonance frequencies at 56.4 Hz, 1021 Hz and 1310 Hz respectively. The transfer functions are presented in Figure 26(a)-25(c).

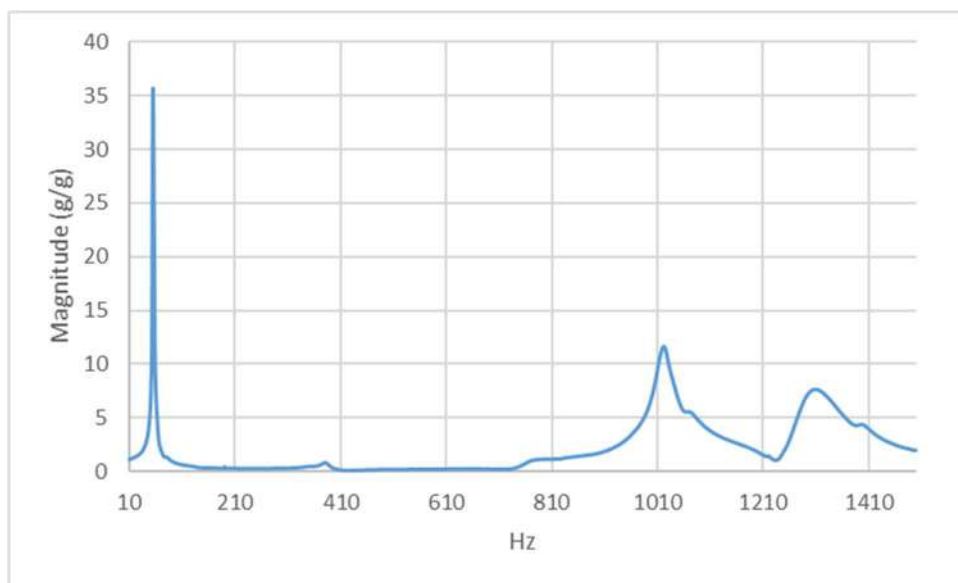
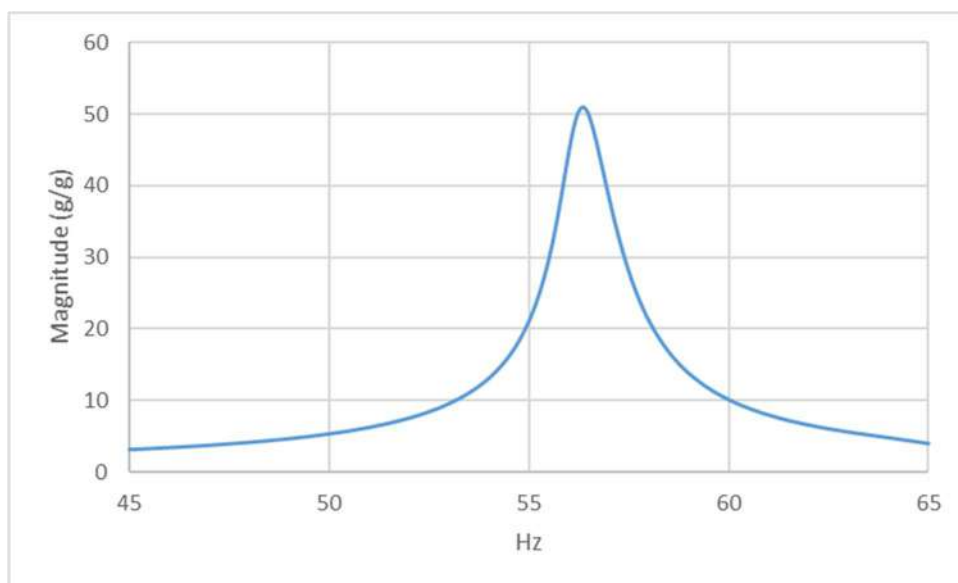
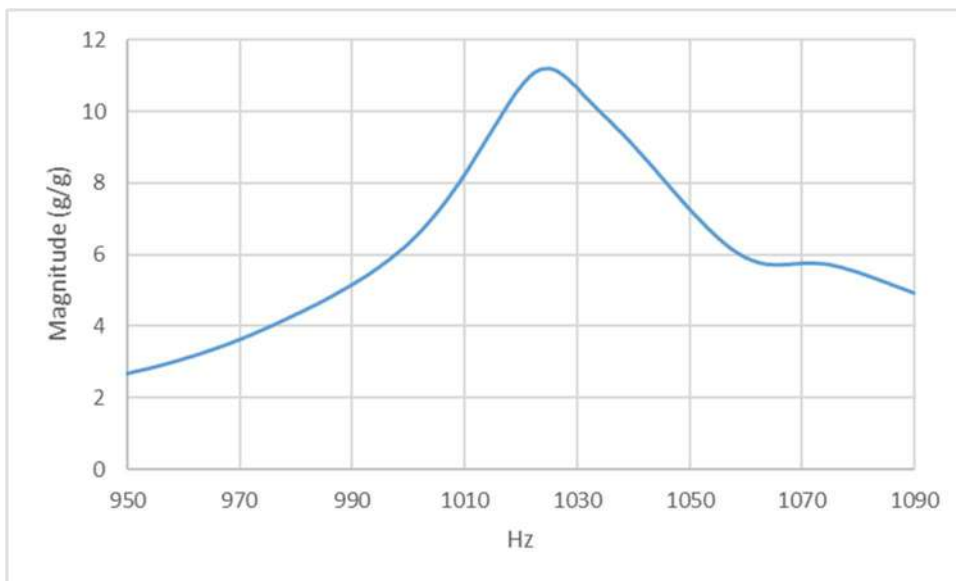


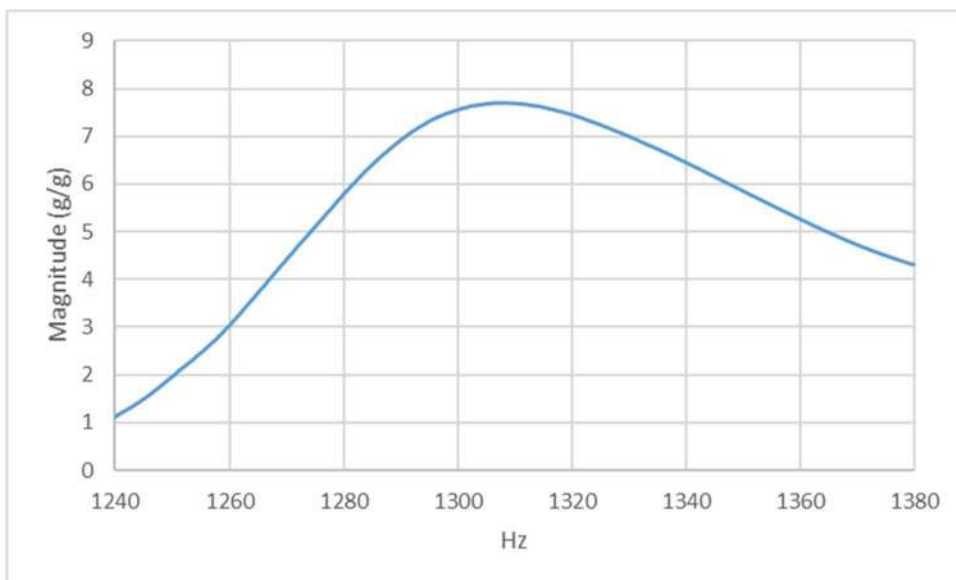
Figure 25. Transfer function for swept sine signal (10 Hz to 1500 Hz)



(a)



(b)



(c)

Figure 26. Transfer function for swept sine signal (a) 45 Hz to 65 Hz; (b) 950 Hz to 1090 Hz; (c) 360 Hz to 400 Hz



4.9 Test on flax/epoxy composite beam 2: Case 2

This test was conducted on the flax/epoxy composite beam 2. The accelerometer was attached to the specimen at 0.2l distance (23.4 mm) from the clamped end to measure the dynamic response of the beam as shown in Figure 27. Another sensor was mounted to the shaker to control the excitation of the shaker.

The vibration signal was swept from 10 to 1500 Hz with 750 data points (linear distribution). The transfer function is presented in Figure 28. The resonance frequencies are identified at 61.7 Hz, 378 Hz, 993 Hz and 1300 Hz. Following the full-range scan, in order to measure the resonance frequencies more accurately, several scans were conducted around range of each resonance frequency. The frequency ranges are as follows: 50-70 Hz (200 data points), 360-400 Hz (200 data points), 950-1050 Hz (400 data points), and 1250-1350 Hz (400 data points) with resonance frequencies at 62.9 Hz, 377 Hz, 995 Hz and 1300 Hz respectively. The transfer functions are presented in Figure 29(a)-28(d).

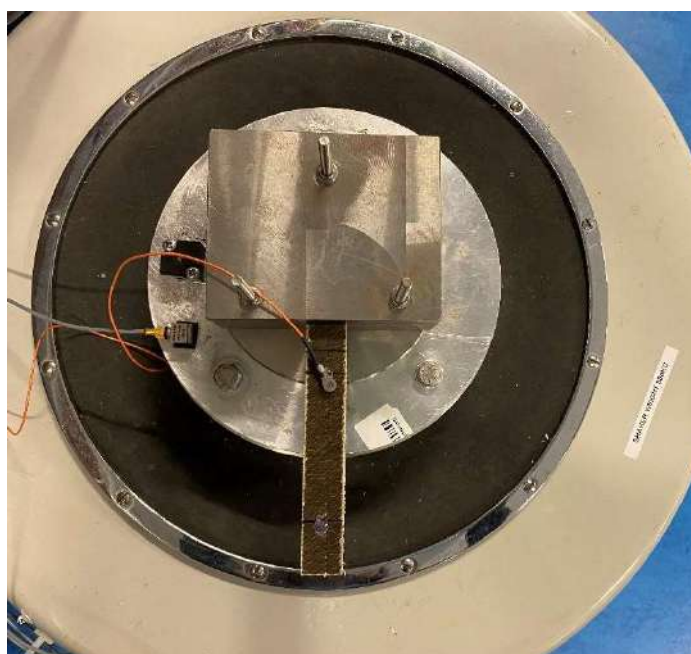


Figure 27. Experimental setup for flax/epoxy composite beam 2: Case 2

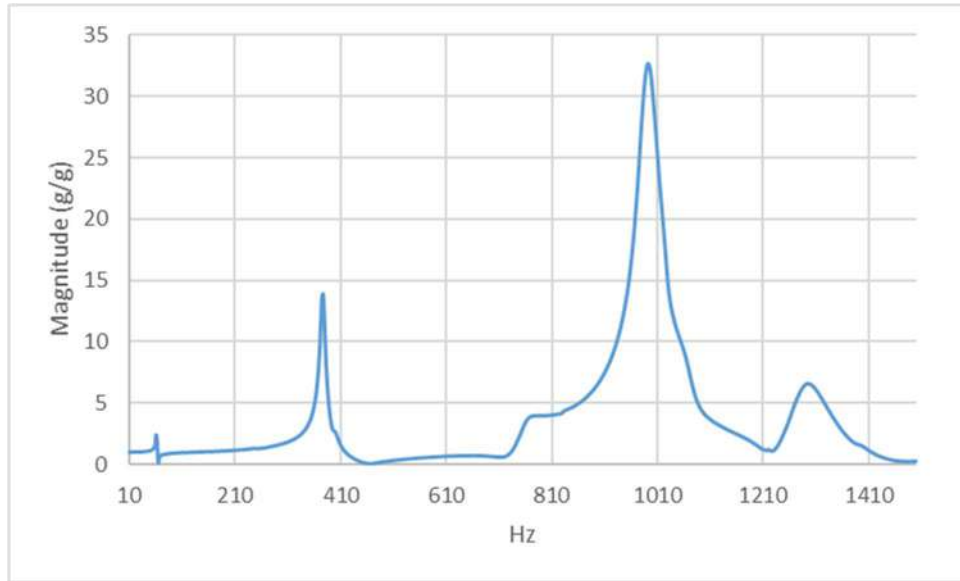
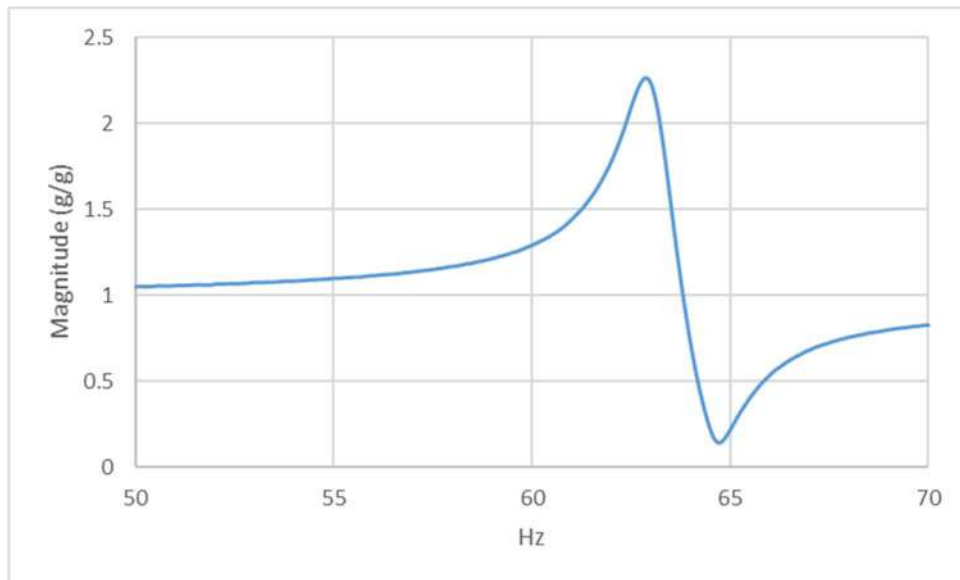
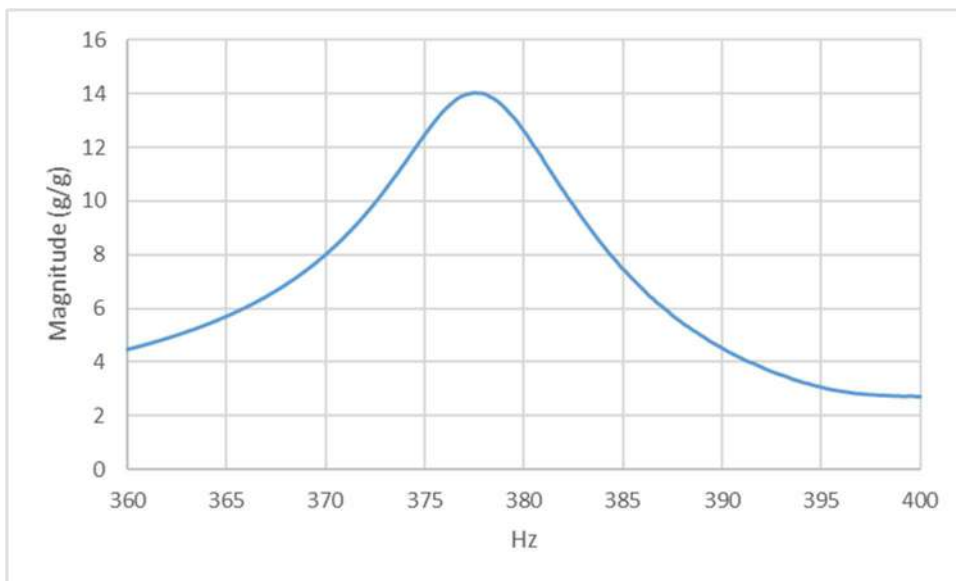


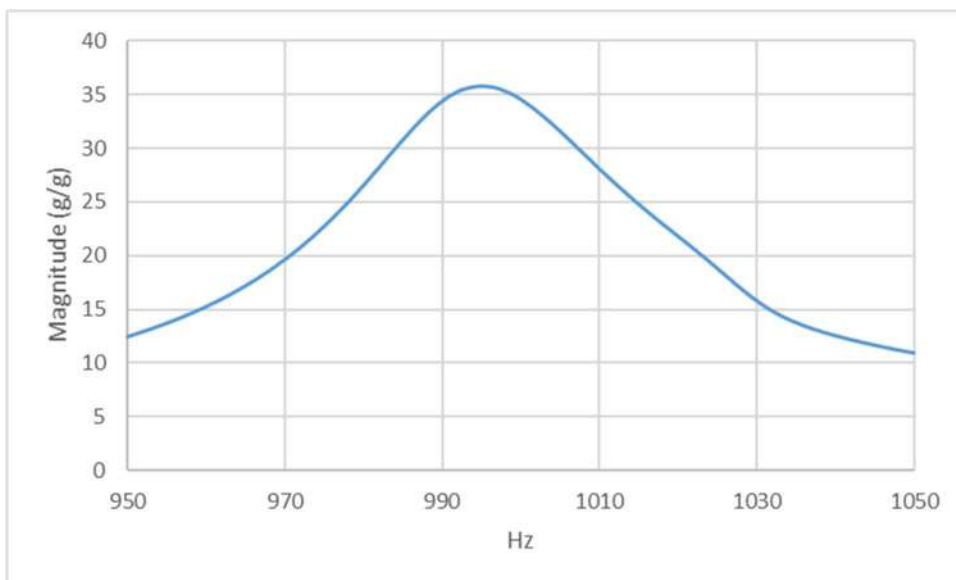
Figure 28. Transfer function for swept sine signal (10 Hz to 1500 Hz)



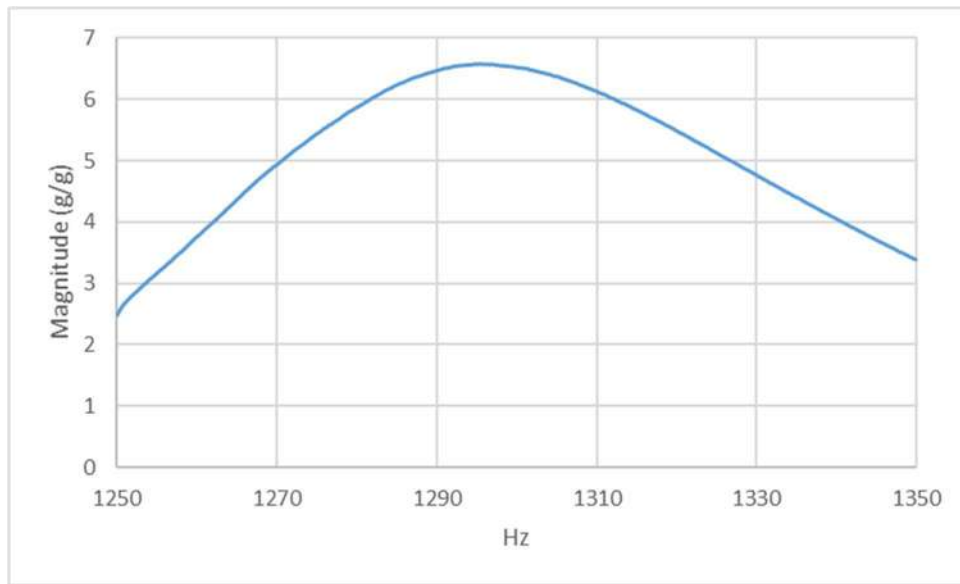
(a)



(b)



(c)



(d)

Figure 29. Transfer function for swept sine signal (a) 50 Hz to 70 Hz; (b) 360 Hz to 400 Hz; (c) 950 Hz to 1050 Hz; (d) 1250 Hz to 1350 Hz



The mode shapes obtained from FEM are presented in Figure 30.

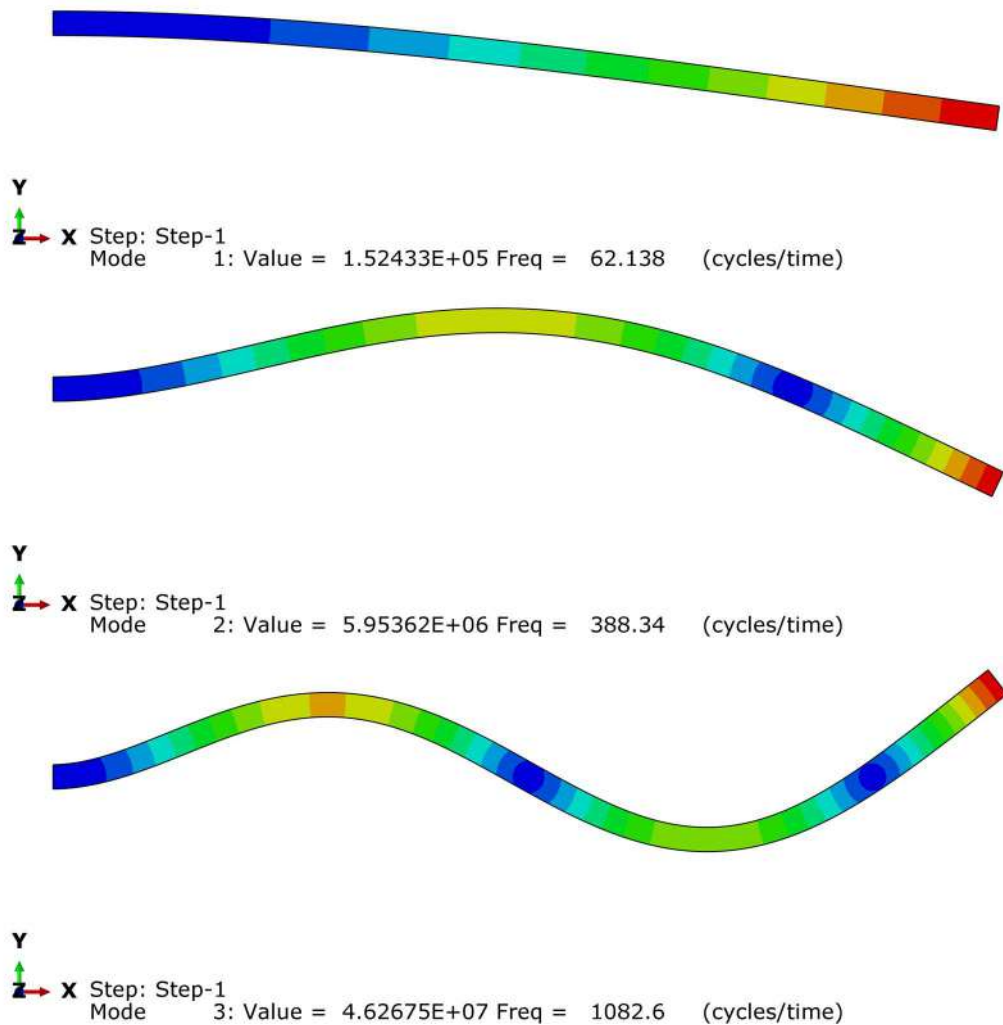


Figure 30. First three frequencies of vibration for flax/epoxy composite (beam 2) calculated by Abaqus

FEM



4.10 Test on flax/carbon hybrid composite beams (2nd batch of samples)

These set of experiments were conducted on the flax-carbon/epoxy hybrid composite beams with 11 different fibre layup schemes. The first nine configurations are labelled in alphabetical order from A to I. Also, configurations Y and Z are suggested as reference specimen types. The layups of each specimen are shown in detail in Appendix A.

The detailed parameters of the materials are listed in Table 7. The accelerometer was attached to the specimens at 0.3l distance from the clamped end to measure the dynamic response of the beam as shown in Figure 31. Another sensor was mounted to the shaker to control the excitation of the shaker.

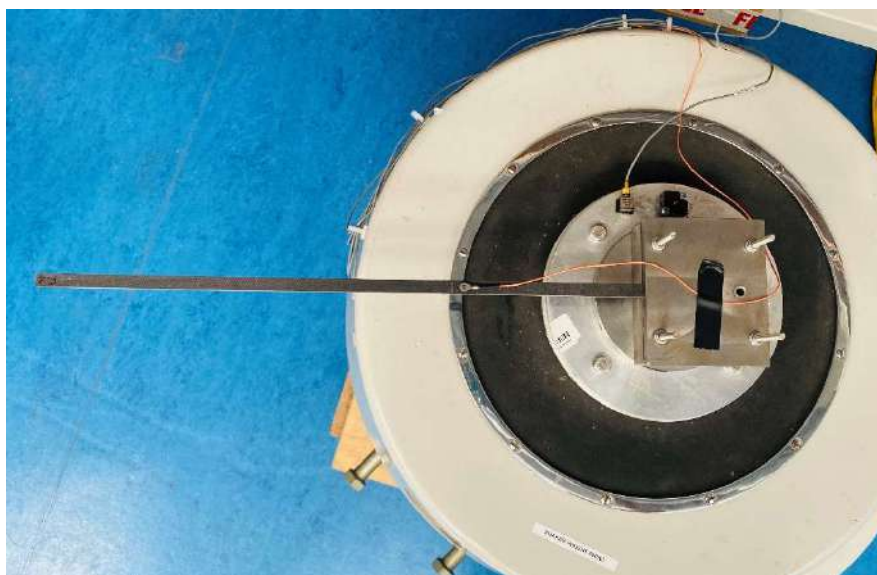


Figure 31. Experimental setup for 2nd phase of tests

The vibration signal was swept from 10 to 1000 Hz with 400 data points (linear distribution). The typical transfer function for the samples from each group is presented in Appendix B. Following the full-range scan, in order to measure the resonance frequencies more accurately, several scans were conducted around range of each resonance frequency. The resonance frequencies are presented in Table 6 and compared with those obtained from analytical and numerical solutions. The mode shapes for the first resonance frequencies of each group of samples obtained from FEM are presented in Appendix C.



Table 7. Resonance frequencies of different laminates obtained from experiment and numerical analysis

Sample	Resonance frequency (Hz)								
	Experimental			Analytical			FEA		
	1 st	2 nd	3 rd	1 st	2 nd	3 rd	1 st	2 nd	3 rd
A1	32.2	200	545	32.4	203	569	32	200	561
A4	31.7	195	528						
B2	30.4	186	502	32.9	206	579	33.2	208	582
B3	29.5	183	499						
C1	26.4	163	447	34.7	217	609	34	213	596
C4	26.5	163	446						
D1	27.4	168	453	30.5	191	535	30.2	189	529
D3	28.8	176	475						
E2	31.9	197	531	31.1	195	546	30.4	190	532
E3	31.9	197	531						
F2	34.3	211	569	31.2	196	547	30.5	191	534
F4	33.8	208	559						
G1	33.7	204	556	33.2	208	583	32.7	204	572
G3	33.5	209	567						
H3	30.4	189	517	32.0	200	562	31.3	195	548
H4	31.9	198	539						
I3	32.3	199	539	32.6	204	572	31.8	199	556
I4	31.9	198	536						
Y1	49.9	316	863	55.3	336	970	57.9	361	1008
Y2	51.4	317	863						
Y3	48.8	305	860						
Y4	49.6	314	860						
Z1	32.3	197	530	26.5	166	465	25.5	160	447
Z3	31.2	193	525						
Z4	31.5	193	524						



The damping ratio and the loss factor obtained from the experiment are presented in Table 8. A comparison of the same is also presented in Figure 32.

Table 8. Damping ratios and loss factor calculated by 3dB method for different laminates

Sample	Damping ratio (%)	Loss factor (%)
A1	0.28	0.55
A4	0.28	0.56
B2	0.25	0.50
B3	0.25	0.49
C1	0.24	0.48
C4	0.24	0.48
D1	0.18	0.36
D3	0.17	0.34
E2	0.25	0.50
E3	0.22	0.44
F2	0.24	0.47
F4	0.24	0.48
G1	0.24	0.48
G3	0.24	0.48
H3	0.26	0.52
H4	0.25	0.50
I3	0.21	0.41
I4	0.21	0.42
Y1	0.75	1.50
Y2	0.77	1.54
Y3	—	—
Y4	0.76	1.52
Z1	0.20	0.40
Z3	0.21	0.41
Z4	0.21	0.41

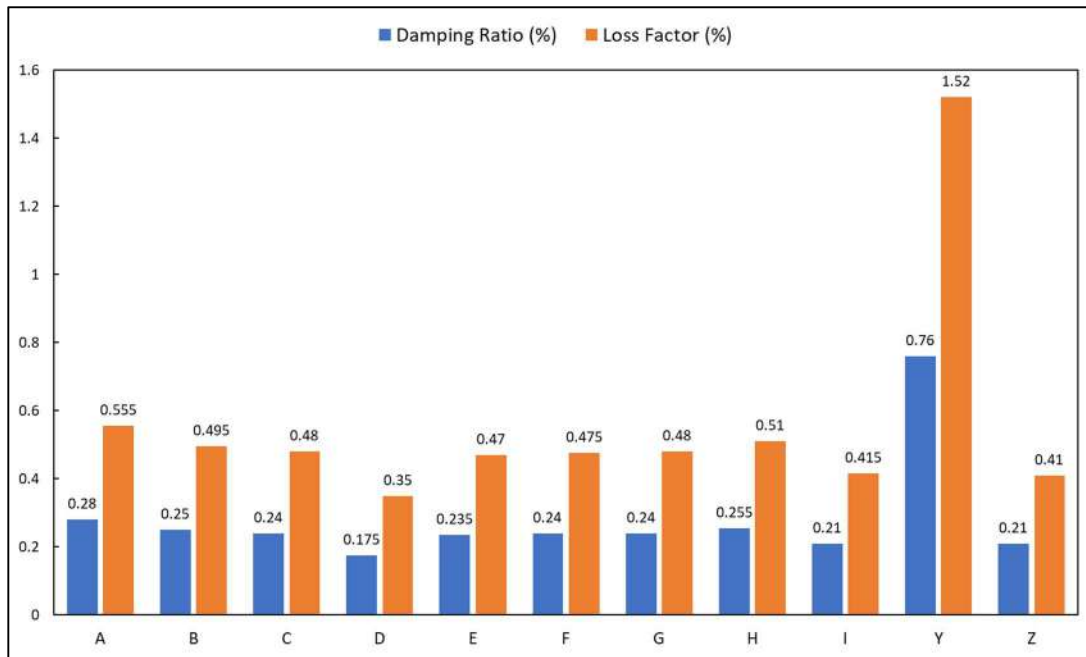


Figure 32. Comparison of damping ratio and loss factor for different samples (for configuration details, refer to Appendix A)

It is observed from the experimental outcome that the fundamental frequency of the hybrid flax/carbon composite material higher than that of flax/epoxy composite laminate. The presence of carbon fibre in the hybrid composite increases the stiffness of the laminate which in turn increases the fundamental frequency.

From the parametric study, conducted in section 4.10, it is observed that the resonance frequencies obtained from the experiments are in good agreement with those obtained from the numerical solution. It can be observed from Table 7 that the reference flax sample (Y) has highest damping ratio which can be attributed to the higher damping properties of flax fibre because of its morphological structure. However, since the number and position of the carbon plies and the flax plies (both UD and non-UD) vary inconsistently throughout the laminates, making an overall comparison about the effect of each parameter (position and number of flax layers) on vibrational behaviour of the samples does not give significant conclusive remarks.

On the other hand, by dividing the samples in different groups based on the position, number and orientation of the flax and carbon layers can give some interesting observations. A comparison between the damping ratio of samples A, C and H shows that the increased number of flax layers improves the damping properties of the laminate. The damping ratio is

increased for unidirectional orientation of flax fibre (sample A) by 33.33% from 90° orientation of flax fibre (sample I) and by 27.27% from +/- 45° orientation (sample E) of flax fibre. It is also observed from the comparison of samples F and G that the orientation of the flax fibre does not seem affecting the damping properties if the number and position of the layers are kept constant. The comparison between samples B and F shows that the position of the flax layer plays an important role in the damping behaviour of the laminates. Placing the flax ply in the outer layer (sample B) increases the damping ratio by 4.2%, inspite of the fact that there are more flax layers in sample F. However, the similar trend is not followed by the flax layer with +/- 45° orientation. It is observed from the comparison of samples D, E and G that the damping ratio is less for sample D where the flax ply (+/- 45°) is placed on the top layer of the laminate.

Dynamic characteristics indicate that flax fibre composites can successfully be applied over the low and broader frequency range. A significant increase in damping is feasible in flax fibre composites compared to more widespread composite materials, for example, glass or carbon fibre reinforced epoxy composites.

The embedding of flax fibres in the polymeric matrix provides considerable damping with a reasonable stiffness. Thus, these make them an excellent candidate for light-weight structural applications. Potential applications may be considered in areas where significant damping is required, for example, automobiles, aircraft interiors, machinery parts, sporting goods and musical instruments. The benefits of having high loss factors with lightweight flax fibre reinforced composites are prolonged service life of the composite parts, reduction in noise and vibration, reduction in the effect of dynamic loading on the structural response, and decrease in weight. Therefore, if certain structural requirements (for example, high stiffness or high impact strength and damping) need to be met, flax fibre composites can be a viable candidate.

An overall good agreement between experimental and analytical solutions is found for most specimen types. However a difference is detectable, especially for specimens C and Z. One reason for such differences can be due to the high thickness to width ratio of specimens which makes the Euler-Bernoulli theory to be less accurate.



5 Conclusions

The present work investigated the effects of fibre orientations and carbon fibre hybridisation on the vibration damping behaviour of different types of flax fibre reinforced epoxy composite and its carbon fibre hybrid laminates provided by the industrial partner, Kairos. The experimental tests were first carried out in order to determine the natural frequency and damping ratios. Then numerical estimates of the response, and in particular the natural frequencies, were made using a finite element model. The numerical modelling showed good agreement with the experimental results. Finite element analysis provided detailed results on the layer by layer influence on the overall natural frequency of investigated composites. It was observed that composite with flax fibre placed outer layer provided the highest damping ratio except for laminates with orientation $\pm 45^\circ$. This indicated that flax epoxy composites performs better in terms of providing better damping reation compared to carbon fibre/flax hybrid composites. This is attributed to the energy dissipating capability of flax fibre due its morphological charactersitics. The findings suggest that the reinforcement of flax fibres in the polymeric matrix provides considerable damping properties with a acceptable stiffness.



References

1. James J. Sargianis, Hyung-Ick Kim, Erik Andres, JonghwanSuhr. Sound and vibration damping characteristics in natural material based sandwich composites. *Composite Structures*, 2013(96): 538–544.
2. Dakai Chen, Jing Li, JieRen, Study on sound absorption property of ramie fiber reinforced poly(L-lactic acid) composites: Morphology and properties, *Composites: Part A* 41 (2010) 1012–1018.
3. Rueppel, M.; Rion, J.; Dransfeld, C.; Fischer, C.; Masania, K. Damping of carbon fibre and flax fibre angle-ply composite laminates. *Compos. Sci. Technol.* 2017, 146, 1–9.
4. Le Guen, M.J.; Newman, R.H.; Fernyhough, A.; Emms, G.W.; Staiger, M.P. The damping-modulus relationship in flax/carbon fibre hybrid composites. *Compos. B* 2016, 89, 27–33.
5. Vanwalleghem, J.; de Baere, I.; Huysman, S.; Lapeire, L.; Verbeken, K.; Nila, A.; Vanlanduit, S.; Loccufier, M.; van Paepegem, W. Effective use of transient vibration damping results for non-destructive measurements of fibre-matrix adhesion of fibre-reinforced flax and carbon composites. *Polym. Test.* 2016, 55, 269–277.
6. Dhakal, H.; Zhang, Z.; Guthrie, R.; MacMullen, J.; Bennett, N. Development of flax/carbon fibre hybrid composites for enhanced properties. *Carbohydr. Polym.* 2013, 96, 1–8.
7. Flynn, J.; Amiri, A.; Ulven, C. Hybridized carbon and flax fiber composites for tailored performance. *Mater. Des.* 2016, 102, 21–29.
8. Bos, H.; van Den Oever, M.J.; Peters, O. Tensile and compressive properties of flax fibres for natural fibre reinforced composites. *J. Mater. Sci.* 2002, 37, 1683–1692.
9. Berthelot, J.; Sefrani, Y. Damping analysis of unidirectional glass and Kevlar fibre composites. *Compos. Sci. Technol.* 2004, 64, 1261–1278.
10. Mahmoudi, S.; Kervoelen, A.; Robin, G.; Duigou, L.; Daya, E.; Cadou, J. Experimental and numerical investigation of the damping of flax/epoxy composite plates. *Compos. Struct.* 2019, 208, 426–433.



11. Cheour, K.; Assarar, M.; Scida, D.; Ayad, R.; Gong, X. Effect of stacking sequences on the mechanical and damping properties of flax glass fiber hybrid. *J. Renew. Mater.* 2019, 7, 877–889.
12. Cheung, H.; Ho, M.; Lau, K.; Cardona, F.; Hui, D. Natural fibre-reinforced composites for bioengineering and environmental engineering applications. *Compos. B* 2009, 40, 655–663.
13. Nabi Saheb, D.; Jog, J.P. Natural fiber polymer composites: A review. *Adv. Polym. Technol.* 1999, 18, 351–363.
14. Assarar, M., Zouari, W., Sabhi, H., Ayad, R., & Berthelot, J. M. (2015). Evaluation of the damping of hybrid carbon–flax reinforced composites. *Composite Structures*, 132, 148-154.
15. Mahmoudi, S., Kervoelen, A., Robin, G., Duigou, L., Daya, E., & Cadou, J. (2019). Experimental and numerical investigation of the damping of flax–epoxy composite plates. *Composite Structures*, 208, 426-433.



Appendix A:

In these figures, the lay up for half of the laminate is shown, where the number “1” is representative of upper layer.

1	UD Carbone (300g)
2	UD Flax (200g)
3	UD FlaxTape (110g)
4	UD Carbone (300g)
5	UD Carbone (300g)
6	UD Carbone (300g)
7	UD Flax (200g)
8	UD Flax (200g)
9	UD FlaxTape (70g)
10	UD FlaxTape (70g)

CCCLC UD – A

1	FLAX équilibré
2	UD Carbone (300g)
3	UD Carbone (300g)
4	UD Carbone (300g)
5	UD Carbone (300g)
6	UD Flax (200g)
7	UD Flax (200g)
8	UD FlaxTape (110g)
9	UD FlaxTape (110g)

CCCCL 90 – B

1	UD Flax (200g)
2	UD FlaxTape (110g)
3	UD Carbone (300g)
4	UD Carbone (300g)
5	UD Carbone (300g)
6	UD Carbone (300g)
7	UD Carbone (300g)
8	UD Carbone (300g)
9	UD Carbone (300g)

CCCCL UD – C

1	FLAX +/- 45°
2	UD Carbone (300g)
3	UD Carbone (300g)
4	UD Carbone (300g)
5	UD Carbone (300g)
6	UD Carbone (300g)
7	UD Flax (200g)
8	UD FlaxTape (110g)
9	UD FlaxTape (110g)

CCCCL 45 – D

1	UD Carbone (300g)
2	FLAX +/- 45°
3	UD Carbone (300g)
4	UD Carbone (300g)
5	UD Carbone (300g)
6	UD Flax (200g)
7	UD Flax (200g)
8	UD FlaxTape (110g)
9	UD FlaxTape (70g)

CCCLC 45 – E

1	UD Carbone (300g)
2	UD Carbone (300g)
3	FLAX équilibré
4	UD Carbone (300g)
5	UD Flax (200g)
6	UD Flax (200g)
7	UD Flax (200g)
8	UD FlaxTape (110g)
9	UD FlaxTape (70g)

CCLCC 90 – F

1	UD Carbone (300g)
2	UD Carbone (300g)
3	FLAX +/- 45°
4	UD Carbone (300g)
5	UD FlaxTape (70g)
6	UD FlaxTape (110g)
7	UD Flax (200g)
8	UD Flax (200g)
9	UD Flax (200g)

CCLCC 45 – G

1	UD Carbone (300g)
2	UD Carbone (300g)
3	UD Flax (200g)
4	UD FlaxTape (110g)
5	UD Carbone (300g)
6	UD Carbone (300g)
7	UD Carbone (300g)
8	UD FlaxTape (110g)
9	UD Flax (200g)

CCLCC UD – H

1	UD Carbone (300g)
2	FLAX équilibré
3	UD Carbone (300g)
4	UD Carbone (300g)
5	UD Carbone (300g)
6	UD Flax (200g)
7	UD Flax (200g)
8	UD Flax (200g)

CCCLC 90 – I



1	UD Flax (200g)
2	UD Flax (200g)
3	UD Flax (200g)
4	UD Flax (200g)
5	UD Flax (200g)
6	UD Flax (200g)
7	UD Flax (200g)
8	UD Flax (200g)
9	UD FlaxTape (70g)

Reference Flax – Y

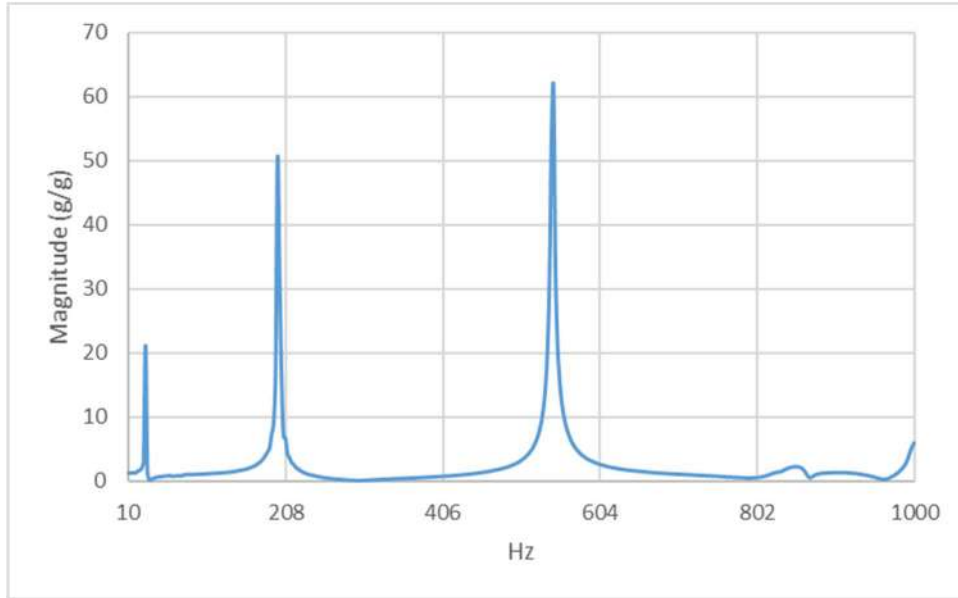
1	UD Carbone (300g)
2	UD Carbone (300g)
3	UD Carbone (300g)
4	UD Carbone (300g)
5	UD FlaxTape (70g)
6	UD Flax (200g)
7	UD Flax (200g)
8	UD Flax (200g)
9	UD Flax (200g)

Reference Carbon – Z

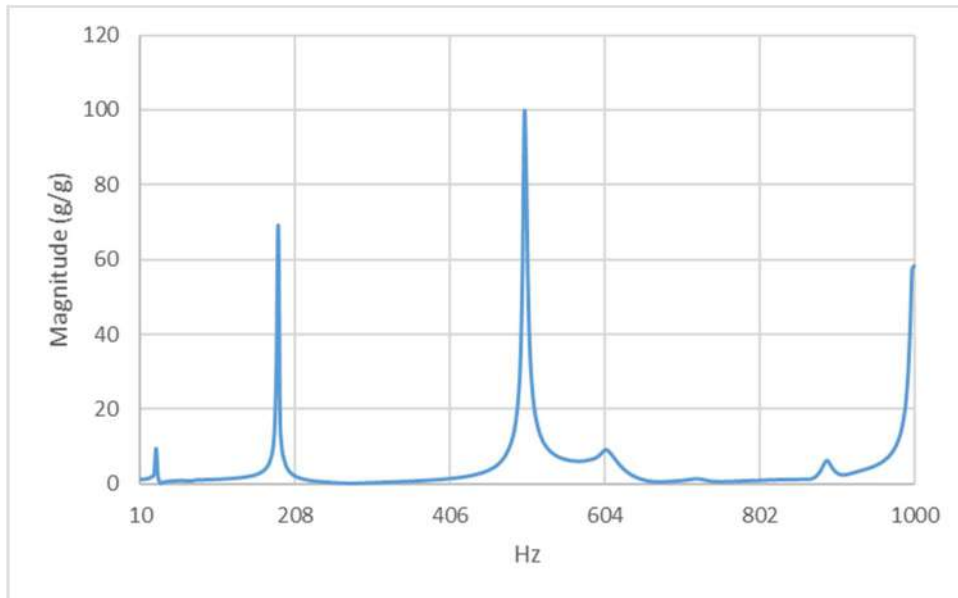


Appendix B:

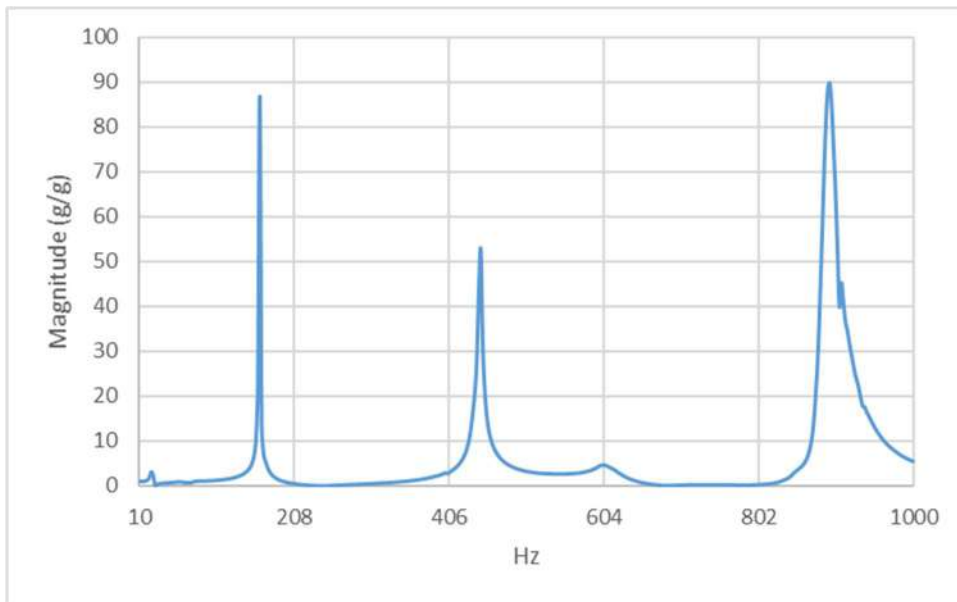
The following figures represent the typical FRF of the flax/carbon epoxy composite samples of each group.



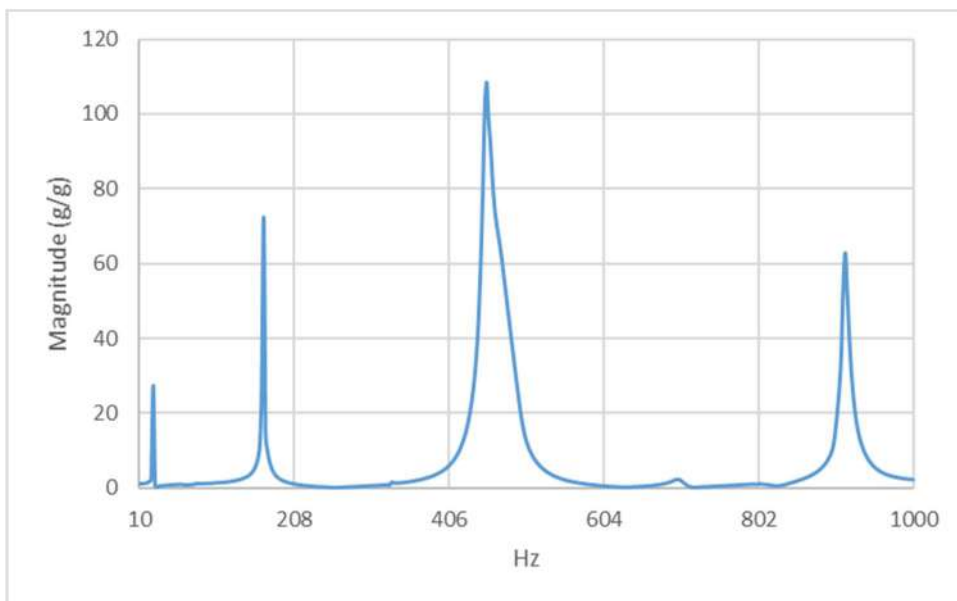
CCCLC UD – A



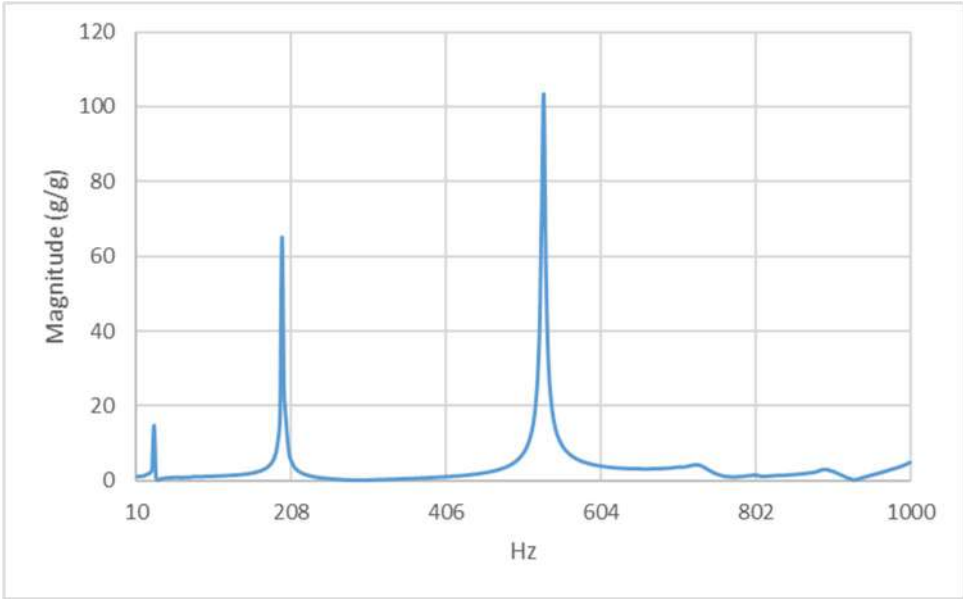
CCCCL 90 – B



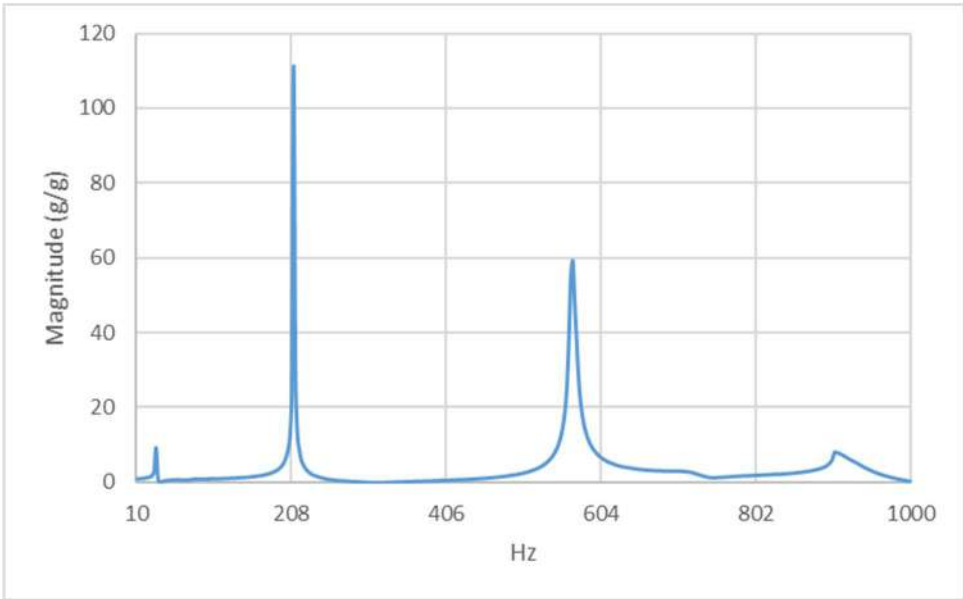
CCCCL UD – C



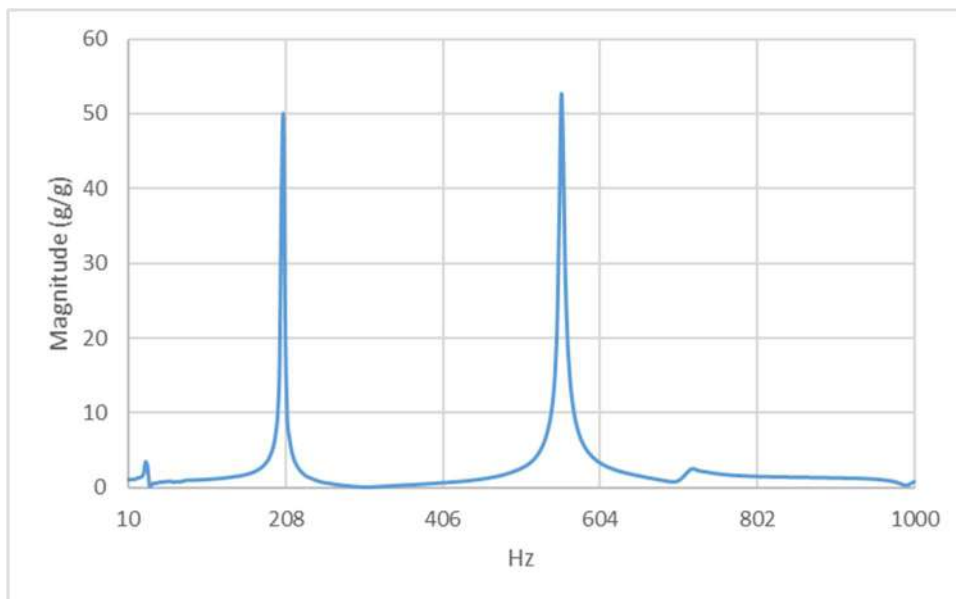
CCCCL 45 – D



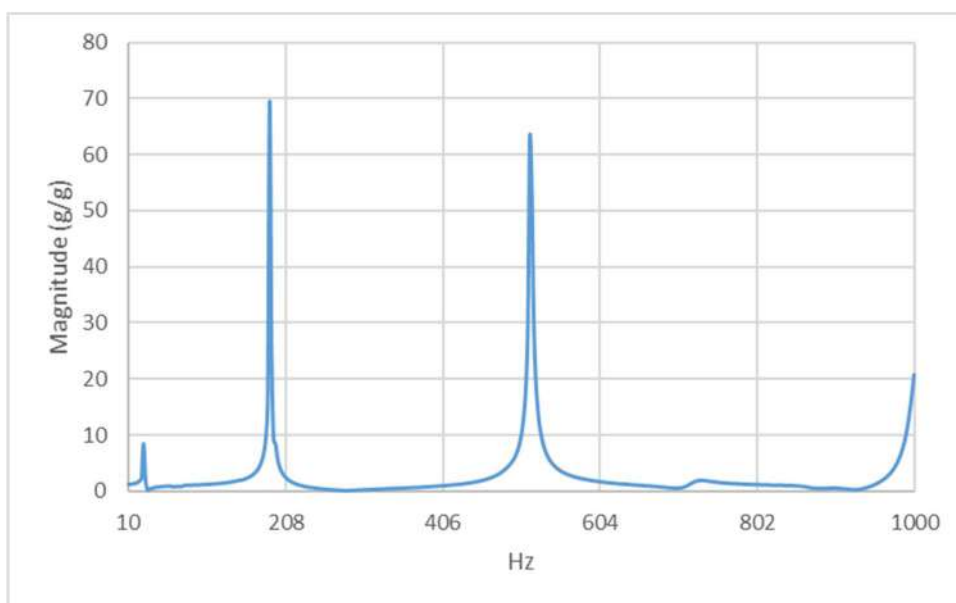
CCCLC 45 – E



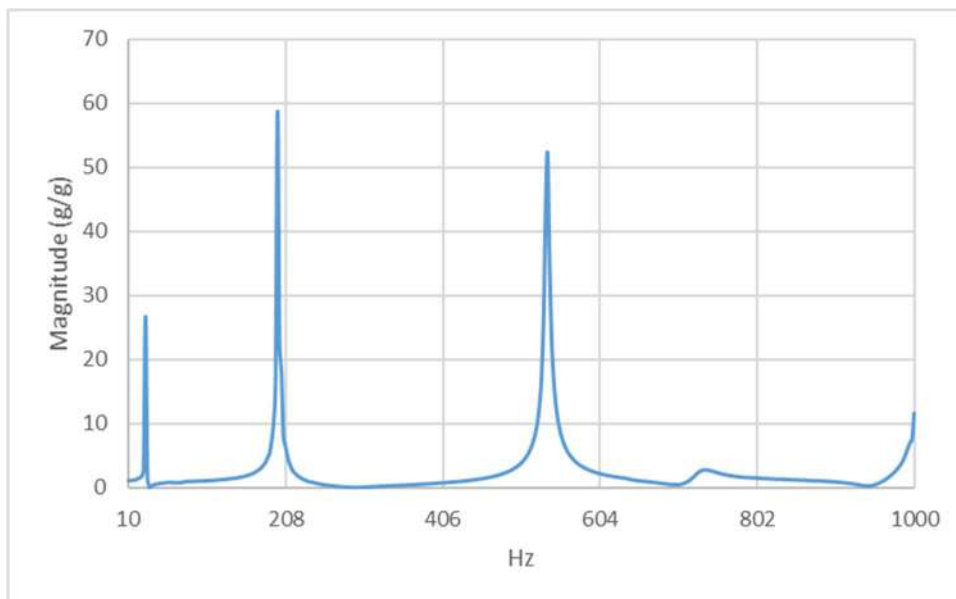
CCLCC 90 – F



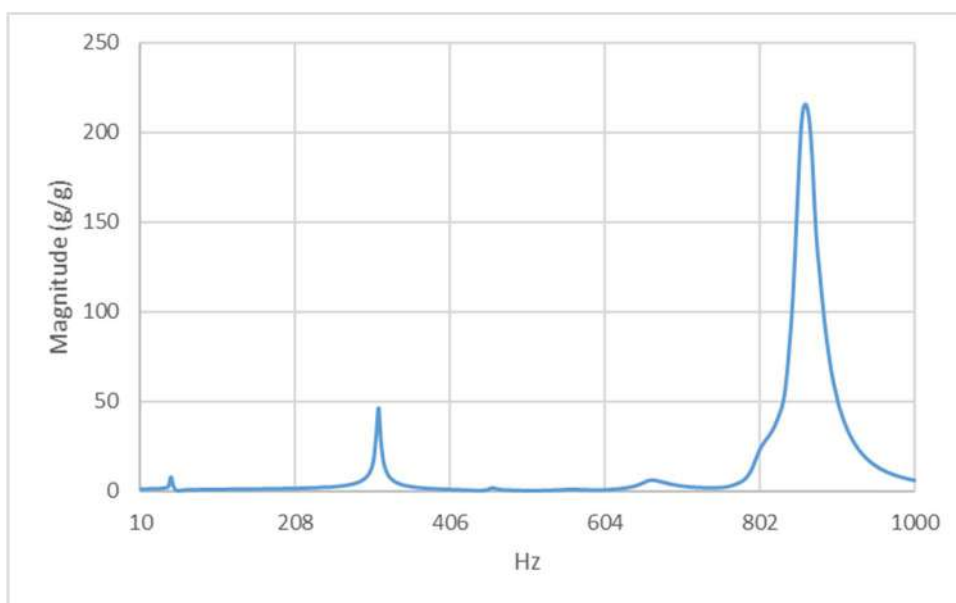
CCLCC 45 – G



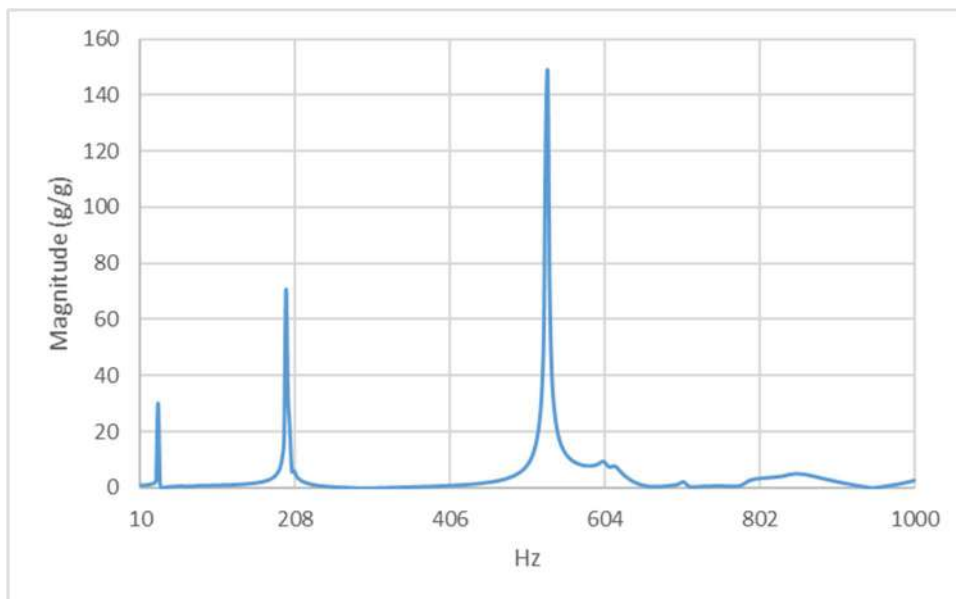
CCLCC UD – H



CCCLC 90 – I



Reference Flax – Y

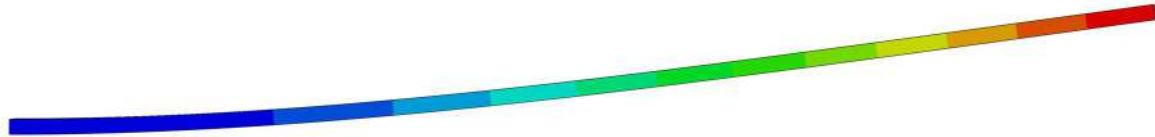


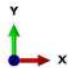
Reference Carbon – Z

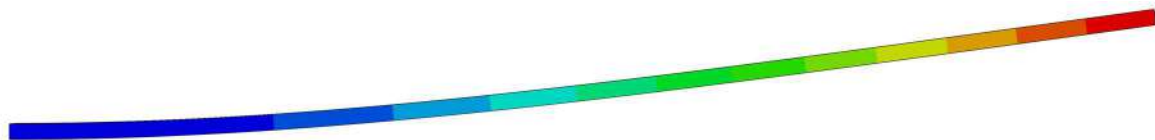


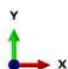
Appendix C:

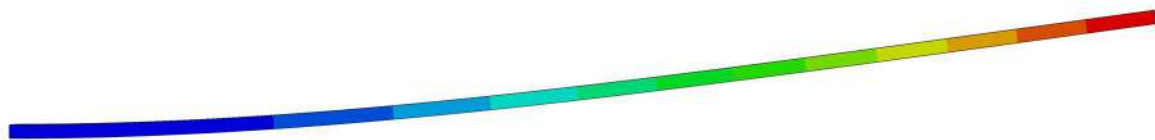
Finite element results for first natural frequency of flax/carbon hybrid composite beams (2nd batch of samples):

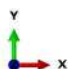


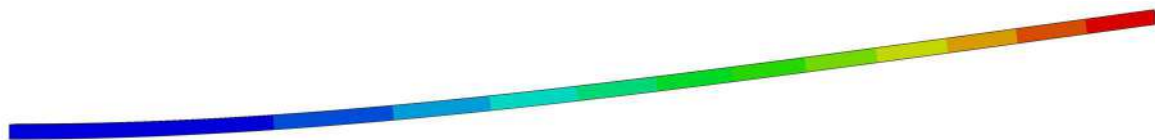

CCCLC UD – A
 Step: Step-1
 Mode 1: Value = 40555. Freq = 32.051 (cycles/time)
 Primary Var: U, Magnitude
 Deformed Var: U Deformation Scale Factor: +1.351e-01

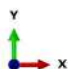


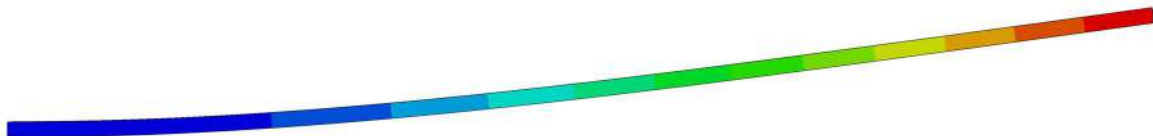

CCCCL 90 – B
 Step: Step-1
 Mode 1: Value = 43618. Freq = 33.239 (cycles/time)
 Primary Var: U, Magnitude
 Deformed Var: U Deformation Scale Factor: +1.405e-01




CCCCL UD – C
 Step: Step-1
 Mode 1: Value = 45752. Freq = 34.043 (cycles/time)
 Primary Var: U, Magnitude
 Deformed Var: U Deformation Scale Factor: +1.360e-01

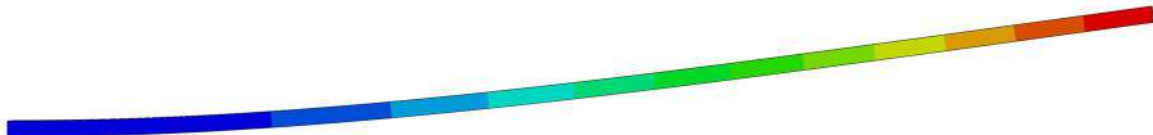



CCCCL 45 – D
 Step: Step-1
 Mode 1: Value = 36044. Freq = 30.216 (cycles/time)
 Primary Var: U, Magnitude
 Deformed Var: U Deformation Scale Factor: +1.363e-01



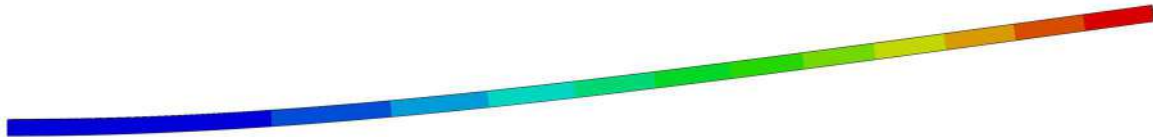
CCLC 45 – E

Step: Step-1
Mode 1: Value = 36562. Freq = 30.432 (cycles/time)
Primary Var: U, Magnitude
Deformed Var: U Deformation Scale Factor: +1.314e-01



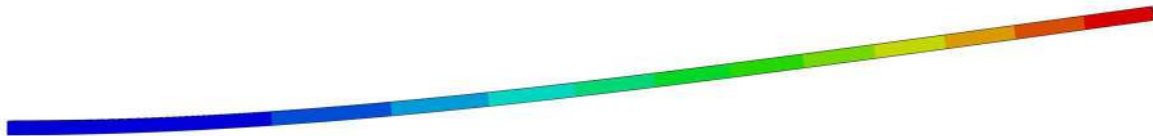
CCLCC 90 – F

Step: Step-1
Mode 1: Value = 36687. Freq = 30.484 (cycles/time)
Primary Var: U, Magnitude
Deformed Var: U Deformation Scale Factor: +1.335e-01



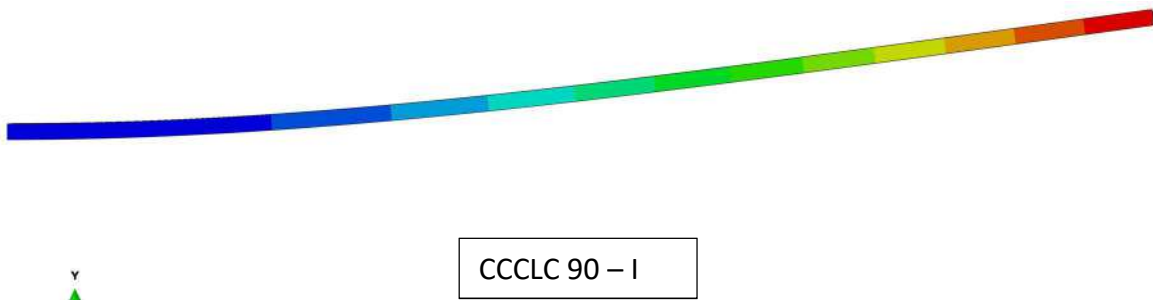
CCLCC 45 – G

Step: Step-1
Mode 1: Value = 42268. Freq = 32.721 (cycles/time)
Primary Var: U, Magnitude
Deformed Var: U Deformation Scale Factor: +1.336e-01



CCLCC UD – H

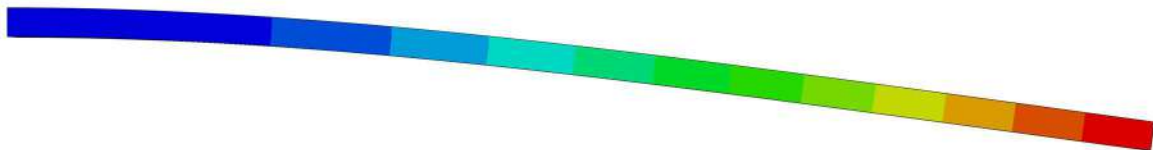
Step: Step-1
Mode 1: Value = 38663. Freq = 31.294 (cycles/time)
Primary Var: U, Magnitude
Deformed Var: U Deformation Scale Factor: +1.263e-01



CCCLC 90 – I



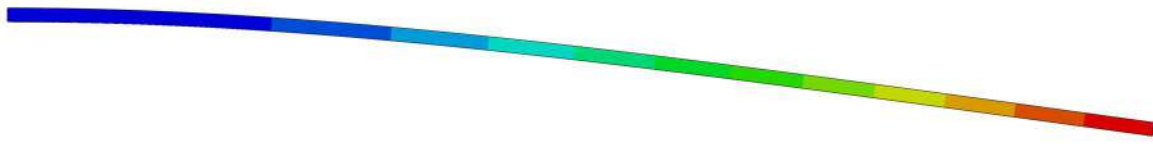
Step: Step-1
 Mode 1: Value = 39930. Freq = 31.803 (cycles/time)
 Primary Var: U, Magnitude
 Deformed Var: U Deformation Scale Factor: +1.333e-01



Reference Flax – Y



Step: Step-1
 Mode 1: Value = 1.32268E+05 Freq = 57.883 (cycles/time)
 Primary Var: U, Magnitude
 Deformed Var: U Deformation Scale Factor: +7.508e-02



Reference Carbon – Z



Step: Step-1
 Mode 1: Value = 25776. Freq = 25.552 (cycles/time)
 Primary Var: U, Magnitude
 Deformed Var: U Deformation Scale Factor: +1.481e-01